Diatom shifts and limnological changes in a Siberian boreal lake: A multiproxy perspective on climate warming and anthropogenic air pollution

Amelie Stieg[1,2], Boris K. Biskaborn[1], Ulrike Herzschuh[1,2,3], Andreas Marent[1], Jens Strauss[1], Dorothee Wilhelms–Dick[4], Luidmila A. Pestryakova[5], Hanno Meyer[1]

[1]Alfred Wegener Institute Helmholtz Centre for Polar and Marine Research, Potsdam, 14473, Germany.
10 [2]Institute of Environmental Science and Geography, University of Potsdam, Potsdam, 14476, Germany.
[3]Institute of Biochemistry and Biology, University of Potsdam, Potsdam, 14476, Germany.
[4]Alfred Wegener Institute Helmholtz Centre for Polar and Marine Research, Bremerhaven, 27568, Germany.
[5]Institute of Natural Sciences, North-Eastern Federal University of Yakutsk, Yakutsk, 677007, Russia.

Correspondence to: Amelie Stieg (*amelie.stieg@awi.de*), Hanno Meyer (*hanno.meyer@awi.de*)

Abstract. Lake ecosystems are affected globally by climate warming and anthropogenic influences. However, impacts on boreal lake ecosystems in eastern Siberia remain underexplored. Our aim is to determine if shifts in diatom assemblages in a remote lake in eastern Siberia are related to climate warming, similar to observations in temperate regions, while also exploring how the ecosystem might be influenced by hydroclimate and human-induced air pollution. We analysed continuous sediment samples from a ^{210}Pb–^{137}Cs–dated short core from Lake Khamra (59.99° N, 112.98° E), covering ~220 years (ca. 1790–2015 CE), following a multiproxy approach on the same sample material to provide a comprehensive record of environmental changes. Biogeochemical proxies include total organic carbon (TOC) and total nitrogen (TN) concentrations and corresponding stable isotopes of bulk sediment samples (δ^{13}C, δ^{15}N), as well as diatom silicon isotopes (δ^{30}Si$_{diatom}$), alongside light microscope diatom species analysis. The diatom assemblage at Lake Khamra is dominated by few planktonic species, primarily *Aulacoseira subarctica* and *Aulacoseira ambigua*. At ca. 1970 CE, we observe a major shift in diatom assemblages, characterised by a marked increase in the planktonic species *Discostella stelligera* and a decrease in both *Aulacoseira* taxa. We attribute these changes to recent global warming, which is likely associated with earlier ice-out and enhanced summer thermal stratification, consistent with similar observations in temperate lake ecosystems. A rapid increase in chrysophyte scales (*Mallomonas*) since the 1990s further supports an increasing thermal stratification of the lake driven by rising temperatures. Biogeochemical proxies indicate substantial limnological changes around 1950 CE, preceding the major shift in diatom communities, likely driven by hydroclimatic variability. Increased precipitation and weathering are further discussed in order to explain changing silica sources leading to decreasing δ^{30}Si$_{diatom}$ after ~1970 CE. Nevertheless, interpretation of δ^{30}Si$_{diatom}$ in lacustrine systems is complex, likely influenced by both in-lake biogeochemical processes and catchment dynamics. Indications of anthropogenic influences on Lake Khamra include a δ^{13}C–depletion, likely linked to fossil fuel combustion and emissions, coinciding with industrial growth in Asia and Russia. Nonetheless, we find no evidence for atmospheric nitrogen deposition. We conclude that the Lake Khamra ecosystem is severely affected by climate warming and shows indications of human influence. This emphasises the urgent need for comprehensive research to mitigate these impacts on remote lake ecosystems in order to secure natural water resources.

1   Introduction

Human activities, particularly the burning of fossil fuels, have contributed significantly to the 'Great Acceleration' of Earth System changes especially since the 1950s (Steffen et al., 2015). Since then, the incidence of major ecological shifts in lake ecosystems globally has increased, driven by both climate change and anthropogenic impacts (Huang et al., 2022). These lake observations align with the proposed onset of the 'Anthropocene' (Crutzen and Stoermer, 2000), though it has not been formally recognised as a distinct geological epoch (ICS, 2024, last access 18. November 2024).

Globally lake surface temperatures have risen in recent decades (O'Reilly et al., 2015; Hampton et al., 2018), having numerous consequences like changing thermal stratification properties, longer ice-free periods and changing lake ecosystems like shifting biological communities (Smol et al., 2005; Saros et al., 2012; Hampton et al., 2017; Woolway et al., 2020). Extensive research on lakes in North America and Europe (Smol et al., 2005; Smol and Douglas, 2007; Rühland et al., 2008; Kahlert et al., 2020) has shown that climate warming and human activities lead to significant ecological changes on remote high latitude ecosystems. In Siberia, for example, Lake Baikal, a thoroughly studied system, has experienced documented ecosystem changes driven by recent warming, including increased water temperatures and shorter ice-cover periods (Todd and Mackay, 2003; Mackay et al., 2006; Hampton et al., 2008; Moore et al., 2009; Hampton et al., 2014; Izmest'eva et al., 2016). However, a notable gap remains in understanding how these global changes impacted boreal lakes in remote and less-studied regions of eastern Siberia, such as the Republic of Sakha (Yakutia).

Yakutia, located in eastern Siberia (Fig. 1a), has experienced rapid climate warming, with annual air temperature trends showing an increase of 0.3 to 0.6°C per decade since 1966 (Gorokhov and Fedorov, 2018). Most meteorological stations report the highest temperature increases in winter, along with a rise in overall precipitation rates over the last 50 years (Gorokhov and Fedorov, 2018). Furthermore, climate warming is associated with an increase in wildfire activity (AMAP, 2021), also observed in Yakutia, which is partly due to anthropogenic alterations to the ecosystems including traditional agro-industrial burning practices and the expansion of industrial areas (Kirillina et al., 2020). Evidence suggests that recent warming and human-induced pollution are impacting limnological conditions in Siberia. For instance, a remote lake in eastern Siberia, without direct human influence in the catchment, displays signs of industrialisation's legacy, with mercury contamination in its sediments and a trend of lake acidification (Biskaborn et al., 2021b).

Diatoms, microscopic unicellular algae prevalent in nearly all aquatic environments, are effective indicators of various environmental disturbances such as climate change, acidification, and nutrient enrichment (Smol and Stoermer, 2010). Their remains, called frustules, are composed of biogenic silica ($SiO_2 * nH_2O$), which are well–preserved in lake sediments. Diatom valves are suitable for light microscopic identification up to the highest species level (Battarbee et al., 2001), as well as for oxygen and silicon isotope measurements to reconstruct past climate and environmental conditions (Leng and Barker, 2006; Sutton et al., 2018; Frings et al., 2024).

Circum–Arctic studies reveal climate warming, resulting in a shortened duration of lake ice covers and an extended growing season, along with thermal stratification of lake water, is the primary cause of observed shift in diatom assemblages (Sorvari et al., 2002; Rühland et al., 2003; Rühland and Smol, 2005; Smol et al., 2005; Rühland et al., 2008; Rühland et al., 2015). Paleolimnological studies in eastern Siberia, including Yakutia, have utilised diatom assemblages, alongside diatom isotopes, biogeochemical proxies such as organic carbon and nitrogen, and mercury analyses to investigate past environmental conditions. However, many of these studies predominantly cover periods within the Quaternary, primarily focusing on the Holocene, and investigate long–term trends (e.g.

Cherapanova et al., 2006; Biskaborn et al., 2012; Pestryakova et al., 2012; Biskaborn et al., 2016; Biskaborn et al., 2021c; Firsova et al., 2021; Kostrova et al., 2021; Mackay et al., 2022; Biskaborn et al., 2023). While there is a growing body of work on recent environmental change in eastern Siberia, high-resolution studies covering shorter

90   time periods in Yakutia remain rare. Besides a study in the remote boreal areas in Yakutia (Biskaborn et al., 2021b), notable study sites are located further south at Lake Baikal (Roberts et al., 2018), on Kamchatka (Jones et al., 2015), further west towards Europe (Palagushkina et al., 2020), or in the northern Urals (Solovieva et al., 2008). However, these sites are influenced by different climatic and ecological conditions that can differ from those in Yakutia.

95   In a previous study at the boreal Lake Khamra in southwest Yakutia, a diatom oxygen isotope record ($\delta^{18}O_{diatom}$) was established to reconstruct hydroclimatic anomalies and suggested increasing (winter) precipitation along with rising air temperatures since the 1970s (Stieg et al., 2024b). In addition to oxygen isotopes, silicon isotopes of diatoms have been used as indicators of changing productivity and nutrient utilization. Predominantly, $\delta^{30}Si_{diatom}$ serves as a proxy for primary production in marine environments (De La Rocha et al., 1998; Sutton et al., 2018).

100   In lacustrine systems, however, $\delta^{30}Si_{diatom}$ interpretation is more complex due to the combined influence of catchment processes (e.g. weathering, vegetation, soil development) and in-lake biogeochemical dynamics (e.g. silica cycling and sedimentation) (Sutton et al., 2018; van Hardenbroek et al., 2018; Frings et al., 2024). Research at Lake Baikal has explored the preservation and reliability of $\delta^{30}Si_{diatom}$ for paleo-reconstructions, as well as its link to diatom productivity and sedimentary processes (Panizzo et al., 2016; 2017; 2018). Despite these studies,

105   spatial and temporal coverage of $\delta^{30}Si_{diatom}$ research in eastern Siberia remains limited. Furthermore, studies that analyse both oxygen and silicon isotopes of diatoms from the same samples are rare, with one example from northern Siberia focusing on the time period since the Last Glacial Maximum (Swann et al., 2010).

In this study, we analyse subfossil diatom assemblages in Lake Khamra to determine whether taxonomic changes are consistent with recent climate warming, as documented in many temperate lakes in North America and Europe.

110   Additionally, we investigate potential limnological responses to climate and anthropogenic impacts. Our research addresses this by examining diatom assemblages and biogeochemical proxies (TOC, TN, $\delta^{13}C$, $\delta^{15}N$, $\delta^{30}Si_{diatom}$) at decadal resolution since circa 1790 CE. Using continuous sediment samples from a short core of Lake Khamra, eastern Siberia, we provide a detailed account of environmental changes. Our specific objectives are to (I) identify historical lake ecosystem changes within a continuous diatom assemblage record spanning the last ~220 years, (II)

115   evaluate the origin of organic material and distinguish between allochthonous and autochthonous sources in response to hydroclimatic variations using biogeochemical proxies, and (III) assess the impact of human–induced air pollution on the lake ecosystem.

2 Materials and Methods

2.1 Study site
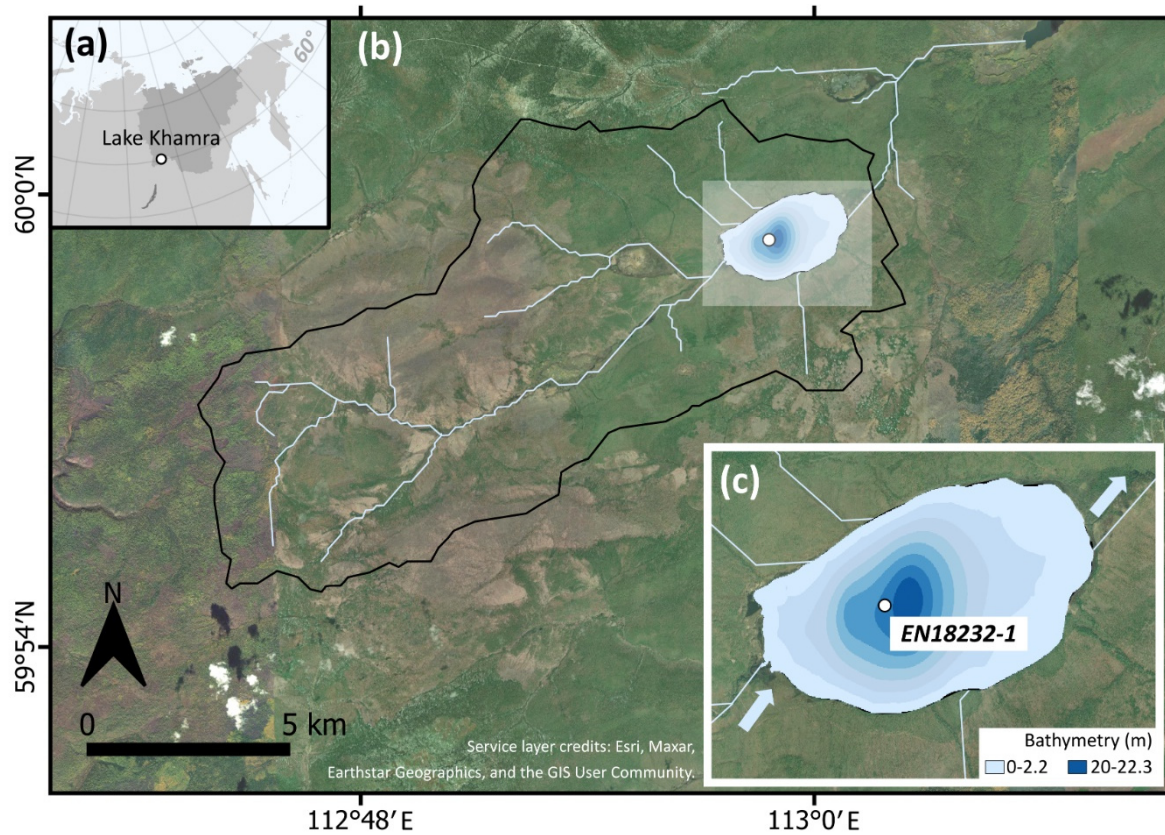
Figure 1. (a) Location of Lake Khamra in eastern Siberia, with Yakutia highlighted in darker grey. **(b)** Catchment of Lake Khamra. **(c)** Bathymetry of Lake Khamra, main inflow in the SW, main outflow in the NE and coring location of EN18232-1 in the central part of the lake. Service layer credits: Esri, Maxar, Earthstar Geographics, and the GIS User Community.

Lake Khamra (59.99° N, 112.98° E, 340 m a.s.l.) is located in the south–west of the Republic of Sakha (Yakutia), eastern Siberia, Russia, with the closest urban settlements, Peleduy and Vitim, situated 40 and 60 km to the south–west, respectively. The landscape is located in the transition zone of evergreen to deciduous needle leaf boreal forest within the ecoregion of the middle taiga (in Geng et al., 2022 after Stone and Schlesinger, 2004). According to field observations (Kruse et al., 2019; Miesner et al., 2022), the research area is covered by a mixed–coniferous forest. The annual mean ground temperature lies between 0.0–1.0 °C at a depth of 10–20 m (Shestakova et al., 2021), indicating that the study site is within a discontinuous to sporadic permafrost zone (Obu et al., 2019). Geologically, the region is underlain by Cambrian bedrock composed of alternating dolomite and limestone, interspersed with silty Ordovician sandstone and patches of clayey Silurian limestone (Chelnokova et al., 1988). The lake morphology is characterised by shallow shore areas and a nearly central deep part with a maximum water depth of 22.3 m (Fig. 1c). The lake has a surface area of 4.6 km² and a catchment size of 107.3 km². Lake Khamra is a hydrologically open system with a main inflow in the south–west and an outflow in the north–east and an estimated average long–term discharge of 1.1 m³ s⁻¹ (Messager et al., 2016). In winter, the lake is covered by ice and snow, observed with an average ice thickness of 0.5 m and an about 1 m thick snow cover in March 2020 (Biskaborn et al., 2021a). Temperatures measured in the water column during that time ranged from 2 to 2.7 °C.

A surface water sample taken during a summer field campaign in 2018 revealed a pH value of 6.07 and a conductivity of 40 µS/cm (Stieg et al., 2024b).

The nearest weather station is located in the town of Vitim (59.45° N, 112.58° E; 186 m a.s.l.; ECA (European Climate Assessment) station code 3235). Details and a climate diagram for the study site can be found in Stieg et al. (2024b). In relation to this, the regional climate is continental, expressed in extremely cold and dry winters (January: -28.8°C mean temp., 1929–2018 CE) and warm and humid summers (July: +18.1°C mean temp., 1929–2018 CE). The annual precipitation average at Vitim reaches 423 mm (1929–2018 CE), while the mean annual air temperature is at -5.0 °C.

2.2   Fieldwork, subsampling and core dating

Coring activities at Lake Khamra were conducted during a summer expedition in 2018 (Kruse et al., 2019). The sediment short core EN18232-1 was obtained with an UWITEC Gravity corer (60 mm) from the central and deepest part of Lake Khamra (59.99091°N, 112.98373°E; 22.3 m), based on water–depth measurements determined with a surveying rope and a portable HONDEX PS-7 LCD digital sounder. The sediment core with a total length of 42 cm was sealed with water-absorbent floral foam and transported in a PVC tube to the Alfred Wegener Institute (AWI) in Potsdam, where it was stored dark and cool at 4°C until further analysis. The sediment core was subsampled downcore in horizontal 1 cm continuous increments (n=39) in October 2021. To avoid potential contamination between depths due to mixing, rim material (<0.5 cm) was carefully removed from each sample layer. All subsamples were freeze–dried for at least 48 h before further processing.

We use the age–depth model for the short core EN18232-1 published by Stieg et al. (2024b), providing a comprehensive ~220–year record (ca. 2015–1790 CE, mean ages) with a sub–decadal resolution according to mean ages (5.7 ± 1.7 years). The chronology relies on analysis for ^{210}Pb, ^{226}Ra, ^{137}Cs, and ^{241}Am using direct gamma assay techniques with Ortec HPGe GWL series well–type coaxial low background intrinsic germanium detectors, conducted at the Liverpool University Environmental Radioactivity Laboratory as described by Appleby et al. (1986). The age–depth model of the short core was calculated with a Bayesian accumulation model within the R package 'rbacon' v2.5.8 (Blaauw and Christen, 2011; R version 4.1.1), based on the ^{210}Pb chronology, shown in Fig. A1 in the appendix. In addition, data on the water content and the average dry bulk density (DBD) of the short core were determined from selected subsamples (n=24) using a 1 cm³ tool taken at regular intervals, with weights measured before and after freeze-drying. The mean DBD (g cm^{-3}) was then used together with the sedimentation rates (SR, cm a^{-1}) to calculate mass accumulation rates (MAR, g cm^{-2} a^{-1}) downcore (full details given in Stieg et al., 2024a).

2.3   Diatom analysis

Diatom slides were prepared for each of the 39 samples of the short core EN18232-1 to analyse the species assemblages. Preparation of slides for siliceous microfossils followed Battarbee et al. (2001). Aliquots of 0.10 g freeze–dried sample material were treated with H_2O_2 (30 %) at 90°C for up to 8 h to remove organic matter. The reaction was stopped and carbonates were eliminated by adding HCl (10 %). After washing with purified water, 5 ml of Microsphere suspension (2 x 10^6 microspheres ml^{-1}) were added to estimate the diatom valve concentration (DVC, Battarbee and Kneen, 1982). In addition, 1 drop of ammonia (NH_3) solution was added to each sample to

prevent clumping of diatom valves. The homogenised sample solution was transferred onto cover slips using Battarbee cups and mounted to slides using Naphrax. A minimum of 350 diatom valves in each sample were counted along transects (mean: 391 valves) by using a ZEISS AXIO Scope.A1 light microscope with a Plan–Apochromat 100x/ 1.4 Oil Ph3 objective at 1000x magnification. Diatom species were identified to lowest possible taxonomic level primarily using classical identification literature (Krammer and Lange-Bertalot, 1991; Krammer et al., 1991; Krammer and Lange-Bertalot, 1997a, b; Hofmann et al., 2011), supported by regional (Russian) floras (Komarenko and Vasilyeva, 1975; Moiseeva and Nikolaev, 1992; Makarova, 2002). Diatom nomenclature and synonyms were applied using online databases such as Diatoms.org (https://www.diatoms.org; last access: 01. August 2024; Spaulding et al., 2021) and AlgaeBase (https://www.algaebase.org; last access: 01. August 2024; Guiry and Guiry, 2024), for some species further supported with input by members of the diatom community online platform DIATOM–L (Bahls, 2015).

In addition, silicified chrysophyte *Mallomonas* scales were counted without further specification to calculate the *Mallomonas* index, which measures *Mallomonas* in relation to diatom cells (M/D), to evaluate the degree of thermal stratification and the trophic status (Smol, 1985; Ginn et al., 2010). The ratio of planktonic–to–benthic diatoms (P/B) of the most abundant species was calculated, excluding tychoplanktonic species, as an additional indicator of paleoenvironmental change. Habitat assignment followed mainly the online database Diatoms.org (https://www.diatoms.org; last access: 01. August 2024; Spaulding et al., 2021) and habitat information from Barinova et al. (2011). Furthermore, the abundances of the dominant *Aulacoseira* species (*A. subarctica* and *A. ambigua*) were summarised to better identify the assemblage changes in relation to the planktonic taxa *Discostella stelligera*.

2.4   Diatom purification process and silicon isotopes

In a previous study (Stieg et al., 2024b), which focused on the oxygen isotopes of diatoms of the sediment short core EN18232-1, a comprehensive description of the diatom isotope purification procedure of the samples is provided. The silicon isotope composition was determined from the same aliquots (Leng and Sloane, 2008). In general, the purification assessment of diatom samples includes wet chemical as well as physical preparation steps (Morley et al., 2004; Leng and Barker, 2006). Essentially, the cleaning procedure included the removal of organic matter with H_2O_2 (30 %), eliminating carbonates by using HCl (10 %) and multiple heavy liquid separations (HLS) with sodium polytungstate solutions (SPT) with decreasing densities (EN18232-1: 2.50–2.12 g cm⁻³) to separate the diatom valves from the heavy minerogenic fraction. High purity of the diatom samples was supported by a contamination assessment using a JEOL M-IT500HR analytical scanning electron microscope (SEM) with an integrated Energy–Dispersive X–ray Spectroscopy (EDS) system.

The laser fluorination method was applied using bromine pentafluoride (BrF_5) as a reagent to completely extract oxygen from the diatom SiO_2 (Clayton and Mayeda, 1963), after employing the inert Gas Flow Dehydration method (Chapligin et al., 2010). The released silicon component combines with BrF_5 to silicon tetrafluoride (SiF_4). The separation of SiF_4 from the bromine compounds was achieved using a cold trap, composed of a slush of ethanol cooled with liquid nitrogen (N_2) at -115 °C. SiF_4 was then transferred and trapped into Pyrex glass tubes for the subsequent silicon isotope analysis (Chapligin et al., 2010; Maier et al., 2013). For all samples (n=39) two SiF_4 extractions were performed (except two samples with only one extraction). The samples were measured 10 times on a MAT 252 IRMS at AWI Bremerhaven against a reference gas with known isotopic composition,

calibrated to the reference quartz standard NBS–28. The data was processed for outliers by performing a Dixon test with a confidence level of 80 % (Dixon, 1953). The results are expressed as delta notation $\delta^{30}Si$ (^{30}Si / ^{28}Si) in per mill (‰). The calibration was done with the internal biogenic silica standard BFC with a known $\delta^{30}Si$ of +0.13 ‰ relative to NBS–28 (Leng and Sloane, 2008). Analytical precision determined by repeated analyses of the internal standard (n=12) was better than 0.07 ‰ (1σ of $\delta^{30}Si$). A weighted mean value for each sample measurement was calculated with a standard deviation resulting from the internal or the external consistency, depending on which value is higher.

2.5   Biogeochemical proxies

The total organic carbon (TOC) and total nitrogen (TN) of 39 samples were determined to analyse historical changes of the organic matter content in the lake sediments. Freeze–dried subsamples were ground to obtain a homogeneous material. TOC was analysed by using an Elementar soli TOC cube. Total carbon (TC) was computed by the sum of TOC and the total inorganic carbon (TIC), published in a previous study (Stieg et al., 2024b). Organic carbon accumulation rates (OCARs, g m^{-2} a^{-1}) were derived by dividing TOC by 100, multiplying it by the mass accumulation rates (MAR) * 10,000 to g m^{-2} a^{-1} unit. TN was quantified by an Elementar rapid MAX N exceed. The measurement accuracy was 0.1 % for both devices, carried out at the BioGeoChemistry Lab at AWI Potsdam. The TOC/TN atomic ratio (C/N), as an indicator of the organic matter source, was calculated by multiplying its mass ratio by 1.167, which is the ratio of the atomic weights of nitrogen and carbon (Meyers and Teranes, 2001). The stable carbon isotope ratio (^{13}C/^{12}C) of all freeze–dried and milled samples was examined, to gain additional information on past productivity and organic matter sources. Prior to isotope measurement, inorganic carbon was removed by a hydrochloric acid treatment (HCl, 1.3 mol L^{-1}). Carbon isotopes were measured by a ThermoFisher Scientific Delta-V-Advantage gas-mass spectrometer equipped with a FLASH elemental analyser EA 2000, a CONFLO IV gas-mixing system and a MA200R autosampler at the ISOLAB of AWI Potsdam. Isotope ratios are given relative to laboratory standards of known isotopic compositions and relative to the Vienna Pee Dee Belemnite (VPDB) reference standard. Nitrogen isotope ratios (^{15}N/^{14}N) of the 39 samples were analysed using the same gas-mass spectrometer and expressed relative to the standard atmospheric nitrogen ratio (air). Both isotope ratios are given as delta notation ($\delta^{13}C$, $\delta^{15}N$) in per mill (‰), with 1σ standard errors better than $\pm$ 0.15 ‰.

2.6   Data processing and statistical analyses

For data processing and statistically analyses, we used the R environment (R Core Team, 2024). Diatom species richness (alpha diversity) and evenness (effective richness) were assessed by calculating Hill's N0 and N2 (Hill, 1973), with a rarefaction of the data set based on the count's minimum (n = 352), to prevent biases of varying sample sizes, utilising the R package 'vegan' (Oksanen et al., 2022). By categorising the diatom counts into dissolved and pristine valves, the *F* index was calculated to assess the diatom valve dissolution (Ryves et al., 2001; after Flower and Likhoshway, 1993) after Flower and Likhoshway, 1993). The *F* index has a total range between 0 and 1, whereby 1 equals a perfect preservation.

For further processing, the total counts of diatom species were converted to percentage data. With the R package 'rioja' (Juggins, 2022) constrained incremental sums–of–squares clustering (CONISS) was performed to define

diatom zones in the record, after square–root transformation and Euclidean dissimilarity calculation of the percentage data of all involved species using the 'vegan' package (Oksanen et al., 2022), to ensure all species contribute meaningfully to the analysis, regardless of their abundance (Grimm, 1987). The diatom relative abundances and CONISS clustering are presented in a stratigraphic diagram using the function 'strat.plot' of the 'rioja' package (Juggins, 2022). The stratigraphy plot displays the predominant species only, which occur at least twice (≥ 2 samples) with a minimum abundance of 2 %.

The length of gradient variation of the percentage data was determined by a detrended correspondence analysis (DCA), calculated in standard deviation units (SD = 1.03), using the 'decorana' function of the R package 'vegan' (Oksanen et al., 2022). Following the thresholds discussed in Birks (2010), a principal component analysis (PCA) was conducted on the most abundant species (≥ 2 % in ≥ 2 samples) after square–root transformation. Additionally, data of diatom isotopes and biogeochemical proxies of the same sediment samples ($\delta^{18}O_{diatom}$, $\delta^{30}Si_{diatom}$, TOC, TN, C/N, OCAR, $\delta^{13}C$, $\delta^{15}N$, mercury, diatom valve concentration, diatom accumulation rates, M/D) were projected onto the PCA ordination plot of diatom data using the 'envfit' function (Oksanen et al., 2022), enabling the visualisation within the taxonomical and ecological context.

Diatom accumulation rates (DAR) were calculated by multiplying the diatom valve concentration (DVC in 10^7 valves g^{-1}) with mass accumulation rates (MAR, g cm^{-2} a^{-1}) according to Birks (2010) and convert it to 10^9 valves m^{-2} a^{-1}.

3   Results

3.1   Diatom assemblages and corresponding indices
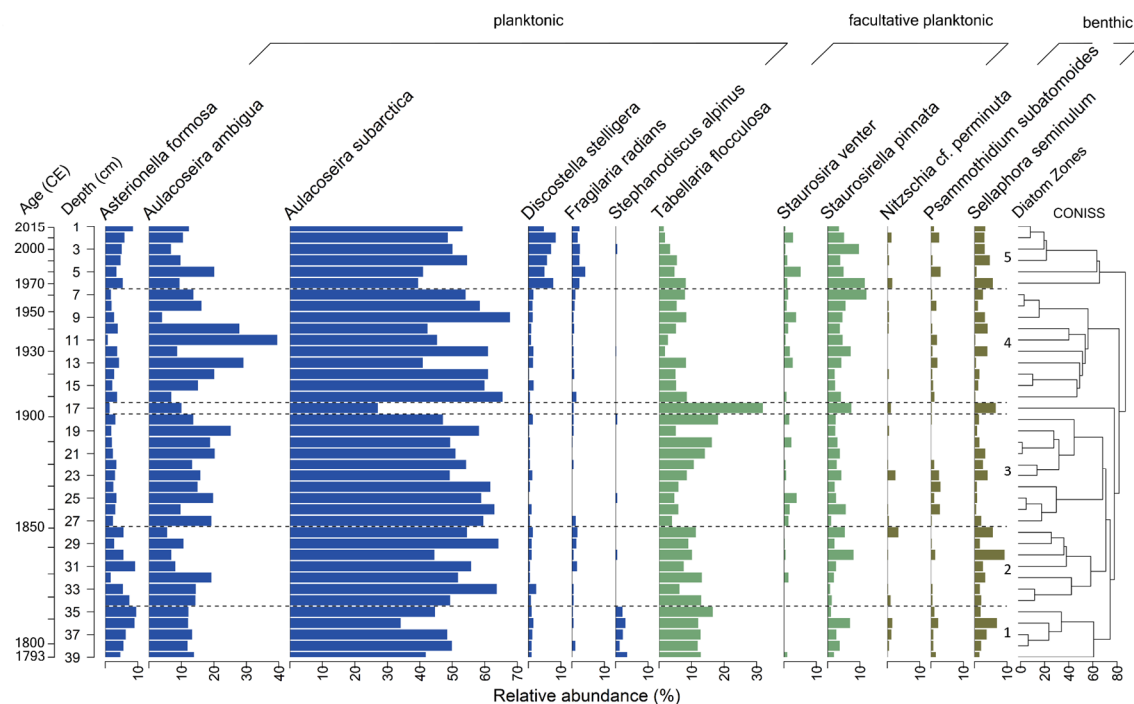
Figure 2. Relative abundances of most dominant diatom species (≥ 2 % in ≥ 2 samples) of the short core EN18232-1 versus sample depth and corresponding mean ages. Diatom zones are based on CONISS clustering shown on the right. Habitat preferences shown at the top.

285 Diatoms occur in all 39 samples of the short core EN18232-1. In total, 102 species were identified, with 12 species occurring with more than 2 % in ≥ 2 samples (Fig. 2). The valve dissolution F index, not displayed here, reveals overall a good valve preservation within the short core (mean: 0.84; min: 0.71; max: 0.92). The record is dominated by the planktonic centric genus *Aulacoseira*, mainly represented by *A. subarctica* and *A. ambigua,* followed by *Tabellaria flocculosa* with a mean abundance of 8.9 %. According to the cluster analysis, we divided the diatom

290 assemblage of EN18232-1 into five diatom zones (Fig. 2). Following percentage values refer to the mean abundance of the individual diatom species within the specific diatom zone. Only the most abundant species (n=12) are considered:

Diatom zone 1 (39–35 cm; circa 1790–1815 CE)

295 The first zone of the diatom record is dominated by the planktonic species *A. subarctica* (43.8 %), followed by the facultatively planktonic *T. flocculosa* (13.2 %) and the planktonic *A. ambigua* (12.7 %). Besides the two *Aulacoseira* species, the planktonic species *Asterionella formosa* (7.0 %), *D. stelligera* (1.2 %), *Fragilaria radians* (0.4 %) and *Stephanodiscus alpinus* (2.5 %) are also represented, at which the latter appears almost only in this diatom zone. Facultative planktonic diatom species are further represented by *Staurosirella pinnata* (3.3 %) and

300 *Staurosira venter,* whereby the latter has only low abundance with a maximum of 1 %. Overall benthic diatoms are the least represented, especially by *Sellaphora seminulum* (3.2 %), followed by *Psammothidium subatomoides* and *Nitzschia cf. perminuta.*

Diatom zone 2 (34–28 cm; circa 1815–1850 CE)

305 Diatom zone 2 is characterised by the two most abundant species *A. subarctica* (54.8 %) and *A. ambigua* (11.3 %), followed by *T. flocculosa* (10.1 %). *A. formosa* (5.4 %) show a slight decrease. Comparable to diatom zone 1, *S. pinnata* (3.2 %) represent facultative planktonic diatoms and benthic diatoms are mainly represented by *S. seminulum* (3.8 %).

310 **Diatom zone 3 (27–17 cm; circa 1850–1910 CE)**

In addition to the almost continuous dominance of *A. subarctica* (52.7 %) and *A. ambigua* (16.4 %), T. *flocculosa* shows an increase (11.4 %) and a peak around 1900 CE at the transition to zone 4 (max: 32 %), while both *Aulacoseira* taxa decline at this point. *S. pinnata* (3.5 %) and *S. seminulum* (2.2 %) also show a slight increase towards zone 4. *A. formosa* (2.6 %) continues to decline, while the facultative planktonic species *S. venter* (1.2 %)

315 appears more frequently in this zone.

Diatom zone 4 (16–7 cm; circa 1910–1970 CE)

Dominant planktonic species are represented by *A. subarctica* (55.7 %) and *A. ambigua* (18.1 %), both reaching a maximum in this zone, while *A. formosa* (2.8 %) stays at a reduced level. Facultative planktonic diatoms are

320 represented rather equally by *T. flocculosa* (5.9 %) and *S. pinnata* (5.1 %), the latter reaching a maximum towards zone 5 (max: 12.0 %). Benthic diatoms, *S. seminulum* and *P. subatomoides* show only minor occurrence.

Diatom zone 5 (6–1 cm; circa 1970–2015 CE)

The uppermost diatom zone is characterised by a decrease of the two dominant *Aulacoseira* species (*A. subarctica*: 47.9 %; *A. ambigua*: 11.5 %) and a clear increase of the planktonic *D. stelligera* (6.5 %) as well as of *A. formosa* (5.5 %) and *F. radians* (2.6 %). The occurrence of *S. pinnata* (6.5 %) remains elevated in this zone. The abundance of *T. flocculosa* (4.1 %) declines towards the top to its lowest values in the record. Benthic diatoms are still underrepresented mainly based on *S. seminulum* (3.4 %).

Indices, derived from the diatom data set, are presented in Fig. 3. The diatom valve concentration (DVC) increases towards the top of the core and range from 82.7 to 533.8 10^7 valves g^{-1}, with a mean of 212.2 10^7 valves g^{-1}. This results in a mean diatom valve accumulation rate (DAR) of 464.1 10^9 valves m^{-2} a^{-1} (200.98–1529.6 10^9 valves m^{-2} a^{-1}). The rarefied species richness, Hill's N0, has a mean of 21.6 and varies between 13.9 and 27.7. The evenness (effective richness), Hill's N2, result in a mean of 3.3 and span from 2.1 to 6.0. The combined abundance of *A. ambigua* and *A. subarctica*, has a mean of 66.7 % and has a similar curve to the ratio of planktonic–to– benthic diatoms (P/B). Downcore the P/B ratio fluctuate along the mean value of 24.6 before it declines to values below the mean after ca. 1950 CE. The *Mallomonas* index (M/D) has a mean of 3.5 and ranges from 0 to a clear maximum of 21.9 in the topmost sample (Fig. 3).
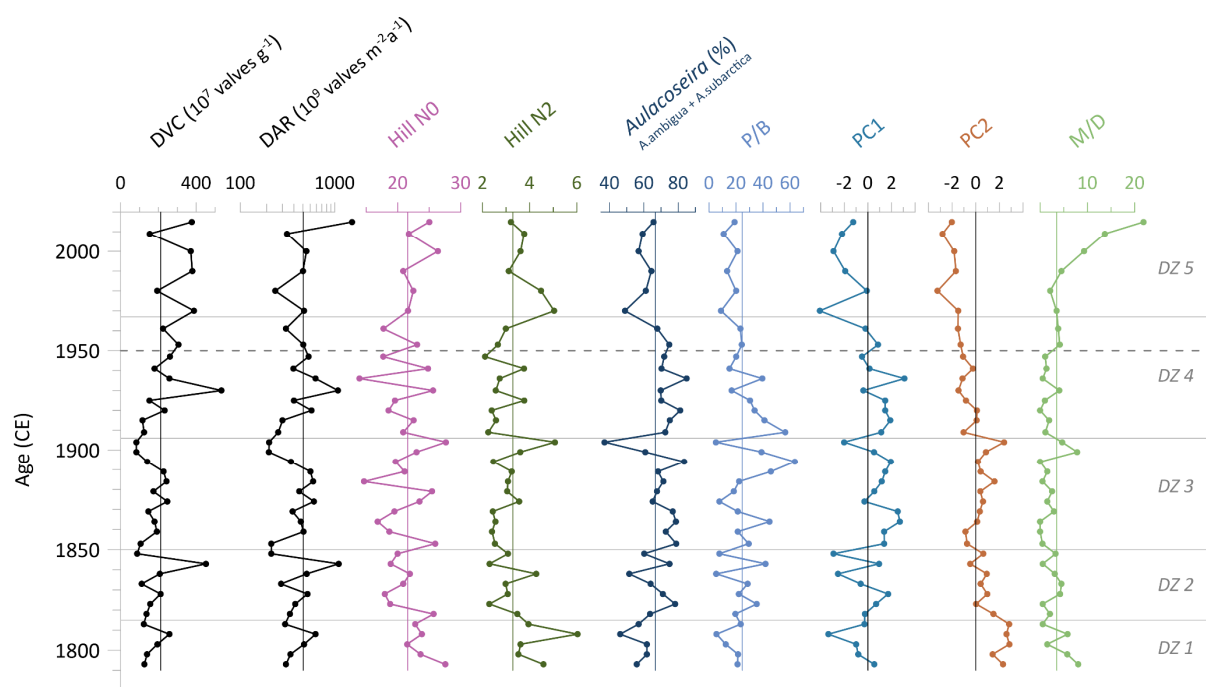
Figure 3. Statistical diatom indices of the short core EN18232-1. Diatom valve concentration (DVC), diatom accumulation rate (DAR), diatom species richness (Hill's N0) and evenness (Hill's N2), abundances of *Aulacoseira* species (*A. ambigua* and *A. subarctica*), planktonic–to–benthic species ratio (P/B) of most abundant species excluding tychoplanktonic species, main axis sample scores of principal component analysis (PC1, PC2), and the *Mallomonas* index (M/D). Vertical lines indicate the mean values. Horizontal lines indicate diatom zones (DZ), the dashed line marks the time before and after 1950 CE.

The biplot of sample scores on the first and second axes of the principal component analysis (PCA) of diatom species data explains nearly 45 % of the total variance, whereby PC1 explains 25.7 % and PC2 explains 19.2 % (Fig. 4). TOC, TN and the *Mallomonas* index (M/D) show association with the diatom species *S. pinnata* along the negative axis of PC1 and PC2 and with diatom samples after 1950 CE. Mercury, measured at the same sample material (Stieg et al., 2024b), is affiliated with the diatom species *D. stelligera* and *F. radians* and also points

towards samples after 1950 CE. In addition, DVC and DAR point in the same direction, but are both somewhat shorter. The C/N ratio, $\delta^{30}Si_{diatom}$ and $\delta^{13}C$ display opposing clustering to the previous sediment proxies along positive PC1 and PC2 axis. $\delta^{15}N$ is associated with *S. venter* and *A. subarctica* along the negative PC2 axis. OCAR is positioned along the positive PC2 axis, associated with *T. flocculosa* and *S. alpinus*. $\delta^{18}O_{diatom}$ does not exhibit a strong directional association with any particular diatom species.
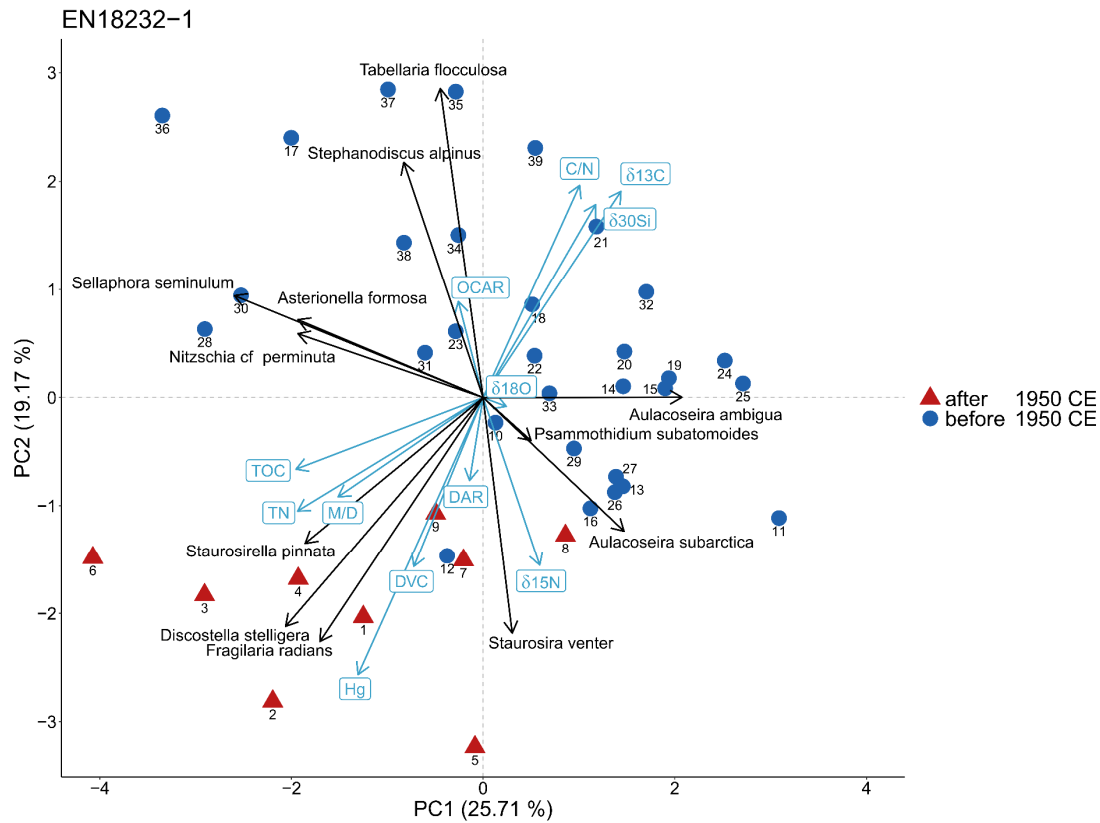
Figure 4. Biplot showing the results of the principal component analysis (PCA) with its first two dimensions (PC1, PC2) of the short core EN18232-1 derived from most abundant diatom species data (≥ 2 % in ≥ 2 samples) and corresponding environmental proxies. The percentage of explained variance for each principal component (PC) is displayed on the axis label. Coloured sample depths indicate mean ages before and after 1950 CE.

3.2   Biogeochemical proxies and $\delta^{30}Si_{diatom}$

The stratigraphic profiles of TOC and TN show a very similar pattern throughout the core (Fig. 5). TOC has a mean value of 9.2 % and TN has a mean of 0.9 %. Around 1800 CE, at the lower part of the core, both proxies are above their mean. Between ca.1830–1940 CE, values decline and stay below their mean, including their minima at about 1875 CE (TOC = 7.5 %, TN = 0.7 %). At the onset of the 1950s, TOC and TN values rise above the mean again and increase nearly continuously since the 1970s, reaching both their total maxima in the uppermost sample (TOC = 12.5 %, TN = 1.2 %). The C/N ratio has a mean of 12.6 and varies by ±1.4. Until the 1950s, the C/N ratio fluctuates slightly between 12.5 and 13, including two maxima at around 1800 CE and 1895 CE. Around 1950 CE, the C/N ratio shifts to lower values of about 12. In the two uppermost samples, the ratio slightly increases again towards 12.5 (Fig. 5). The values of OCAR fluctuate slightly around the mean value of 20.5 g m^{-2} a^{-1} and only fall below it from the 1950s until a minimum of 11.5 g m^{-2} a^{-1} at around 1970 CE, before rising to the maximum value of 50.6 g m^{-2} a^{-1} in the youngest sample (Fig. 5).

$\delta^{30}Si_{diatom}$ ranges between -0.29 to +0.52 ‰, with an overall mean of +0.24 ‰. Until ~1970 CE, $\delta^{30}Si_{diatom}$ values stay mainly above the mean, including the absolute maximum of +0.52 ‰ around 1900 CE. Since the 1970s, $\delta^{30}Si_{diatom}$ values steadily decline and reach the absolute minimum of -0.29 ‰ in the topmost sample (Fig. 5).

380     $\delta^{13}C$ values are mainly above the mean of -30.6 ‰ before 1950 CE, ranging from -31.1 ‰ at about 1800 CE to the absolute maximum of -29.5 ‰ at ca. 1900 CE (Fig. 5). Since the 1950s, $\delta^{13}C$ continuously decreases towards more depleted values, including the absolute minimum of -32.3 ‰ at about 2000 CE. The $\delta^{15}N$ record shows a generally low variability and follows mainly the mean value of +2.9 ‰ and varies in total by ± 0.5 ‰, with slightly enriched values between approx. 1930 and 1970 CE and a subsequent minor decline (Fig. 5).

385
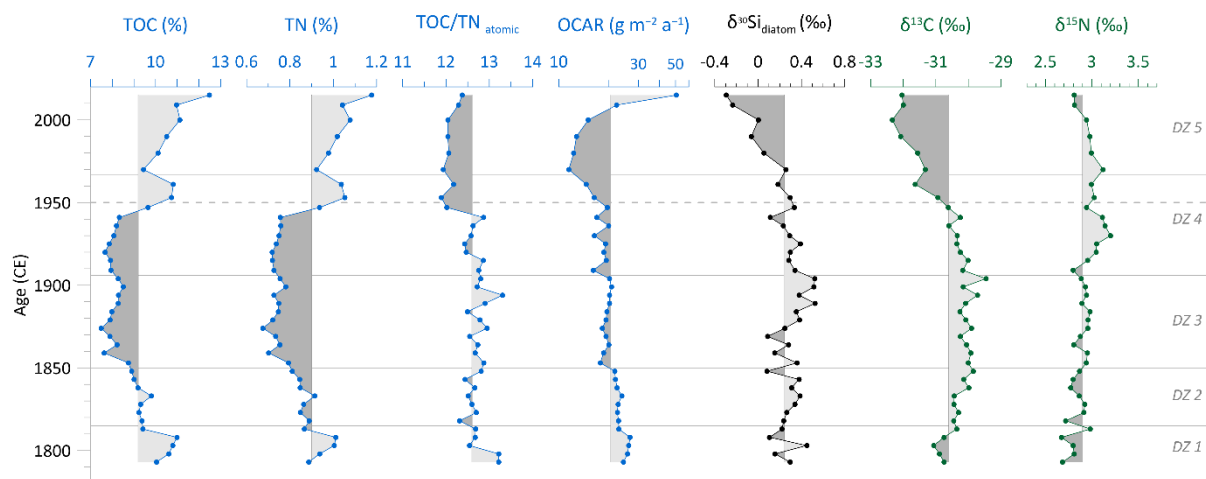
Figure 5. Biogeochemical records of the short core EN18232-1: Total organic carbon (TOC), total nitrogen (TN), TOC/TN atomic ratio (C/N), organic carbon accumulation rate (OCAR), diatom silicon isotopes ($\delta^{30}Si_{diatom}$), as well as stable carbon ($\delta^{13}C$) and nitrogen ($\delta^{15}N$) isotope values of bulk sediment samples. Vertical lines indicate the mean values.
390   **Horizontal lines indicate diatom zones (DZ), the dashed line marks the time before and after 1950 CE.**

4 Discussion

4.1 Limnoecological interpretation of Lake Khamra diatom assemblages

Owing to the deep central part of Lake Khamra (maximum depth: 22.3 m; Fig. 1c), planktonic diatom species have been prominent over the last ~220 years, as reflected by their high abundance within in the short core EN18232-1 (Fig. 2). The planktonic diatom genera *Aulacoseira*, mainly represented by *A. subarctica* and *A. ambigua*, is the most abundant in the sediment record and common in deep, cold, predominantly unstratified lakes in the Arctic tundra (Round et al., 1990; Laing and Smol, 2003). *Aulacoseira* taxa rely on adequate turbulence to stay suspended within the water column (Kilham et al., 1996; Gibson et al., 2003). Thermal stratification or a perennial lake ice cover can weaken the turbulence and lead to a settlement of heavier diatom cells (Gibson et al., 2003). Most *Aulacoseira* species develop dense resting cells as part of their life cycle, which must be resuspended from the sediment into the water column to sustain planktonic populations (Round et al., 1990). Temperature measurements taken under the ice in March 2020 (Biskaborn et al., 2021a) indicate very cold water temperatures at Lake Khamra (mean: 2.5 °C) and a well–mixed water column (Stieg et al., 2024b). Given that *A. subarctica* predominates throughout the record (Fig. 2), it suggests that the growth conditions at Lake Khamra generally favour this species, and a seasonal ice cover does not necessarily reduce its abundance. Furthermore, the snow–rich region and the associated inflow of cold snowmelt water (Stieg et al., 2024b) presumably lead to sufficient turbulence and nutrient upwelling in spring, promoting sustained circulation beneficial for *A. subarctica* (Horn et al., 2011). However, other factors, including atmospheric-surface temperature gradients and wind-induced mixing, are also likely relevant for sufficient lake overturn (Smol and Douglas, 2007; Winder and Sommer, 2012).

Facultative planktonic species, mainly epiphytic (attached to plants), are less abundant and primarily characterised by *T. flocculosa* (reaching up to 32 %) and *S. pinnata* (up to 12 %; Fig. 2). Besides the deep central part, Lake Khamra has a shallow littoral area (Fig. 1c), where macrophytes can provide habitat for epiphytic diatom taxa. Purely benthic diatoms (*N. cf. perminuta, P. subatomoides, S. seminulum*) are of low abundance at Lake Khamra and reach a maximum of 3 % to 9 %. Light limitations due to the lake depth and annual ice cover, cold water temperatures, as well as the availability of nutrients likely regulate the abundance of benthic taxa.

The diatom assemblage of the short core EN18232-1 characterises a deep, open freshwater lake in the boreal forest biome with oligotrophic conditions over the last 220 years. A diatom valve accumulation rate (DAR) consistently above the minimum of 201 $*10^9$ valves m^{-2} a^{-1} indicates continuous diatom accumulation and good preservation environments are reflected by an overall high *F* index (mean: 0.84). These factors, along with the sub-decadal resolution of the record, make Lake Khamra well-suited for paleoecological studies.

4.2 Linking diatom assemblage shifts to hydroclimatic variability

Based on cluster analysis, the diatom assemblage of the short core was subdivided into five diatom zones (Fig. 2). The following discussion focuses on major changes within these zones. In diatom zones 1–4 (pre-1970s), assemblage shifts occur mainly in diatom zone 1 (~1790–1815 CE), followed by a rather stable phase until the 1970s.

From the onset of the record until ~1815 CE, the dominance of the two planktonic diatom species *A. subarctica* and *A. ambigua* was lower than in the subsequent three diatom zones, and remains similarly low as observed in the most recent zone after ~1970 CE (Fig. 3). A hydroclimatic reconstruction from Lake Khamra, based on a

$\delta^{18}O_{diatom}$ record of the same sediment samples (Stieg et al., 2024b), indicates a rather dry and cool period at the onset of the record (~1790–1830 CE). This is reflected in elevated $\delta^{18}O_{diatom}$ values, suggesting reduced winter precipitation (Fig. 6). It is assumed that less precipitation in winter, accumulated as snow, leads to reduced snowmelt water inflow into the lake. This could lead to reduced water turbulence in spring and hence less favourable conditions for *Aulacoseira* to bloom. Both species richness indices (Hill's N0 and N2) are notably higher during *Aulacoseira* reduction, showing a clear distinction between the lowest diatom zone and the subsequent ones. The decline in the dominant *Aulacoseira* species likely reduces competitive pressure, allowing other diatom species to establish and leading to a more diverse diatom assemblage. Noteworthy for the planktonic species is *S. alpinus*, which is primarily present only in the lowermost zone of the diatom assemblage. *S. alpinus* appears in oligotrophic lakes with very low water temperatures (Häkansson and Kling, 1989; Krammer et al., 1991), and this aligns with the assumed cold conditions at the onset of the record. In terms of nutrients, *Stephanodiscus* has a high demand for phosphorus, although it can still grow under low silica concentrations and limited light (Kilham et al., 1986). A reduced meltwater inflow due to overall relatively dry winter conditions could have led to both decreased overturn and a lower input of nutrients, including silica (Si). *Aulacoseira* requires high Si availability for their highly silicified frustules (Laing and Smol, 2003), so a reduction in Si input, combined with weaker turbulence, could have favoured other planktonic species like *S. alpinus* as stronger competitors. Overall, however, diatom accumulation rates (DAR) in the lowest diatom zone are rather low, gradually increasing over time, likely due to the initially cool conditions.

After the dry and cold period at the onset of the record, both *Aulacoseira* species show a clear increase in abundance until the 1940s, reaching their highest abundance of the entire record (Fig. 3). The dominance is accompanied by a decline in effective species richness, as indicated by decreasing Hill's N2 (Fig. 3). The $\delta^{18}O_{diatom}$ hydroclimatic reconstruction suggests a shift from dry to wet conditions around 1830 CE, followed by a prolonged rather stable period in which the lake water was primarily influenced by snowmelt until ~1930 CE (Stieg et al., 2024b). Constant hydroclimatic conditions and sufficient snowmelt input presumably provided lake turbulence in spring and a nutrient upwelling, beneficial for *A. subarctica* (Horn et al., 2011).

Around 1935 CE, *Aulacoseira* reached a maximum in abundance (~ 85 %) but subsequently declined to a minimum of ~50 % at ca. 1970 CE (Fig. 3), reflecting a period of high variability. This corresponds to a phase of hydroclimatic instability, as indicated by meteorological data from the nearest weather station in Vitim, which suggest a prolonged annual precipitation deficit (Fig. 6), particularly in early winter months around the 1950s. This further aligns with a reconstructed dry anomaly in the 1950s based on the $\delta^{18}O_{diatom}$ values (details given in Stieg et al., 2024b) and coincides with increased wildfire activity in the vicinity of the lake, as inferred from a charcoal record from Lake Khamra (Glückler et al., 2021). A reduction of spring overturn, caused by reduced snowmelt water supply, seems a reasonable explanation for the decline of *Aulacoseira*. Comparable to the transition from diatom zone 1 to 2, we observe an increase in diatom species richness and especially in evenness between ca. 1950 and 1970 CE (Hill numbers, Hill's N2 peak in the 1970s; Fig. 3). This pattern coincides with the decline of the dominant *Aulacoseira* taxa, likely allowing other diatom species, like facultative planktonic *T. flocculosa* or *S. pinnata* to compete more successfully.

4.2.1   Diatom shift at ca. 1970 CE: A climate warming signal

The most prominent shift in diatom assemblage occurs around 1970 CE, corresponding to the transition between diatom zones 4 and 5 (Fig. 2). Diatom zone 5 (~1970–2015 CE) is characterised by a substantial increase in the planktonic *D. stelligera*, rising from low relative abundances up to 8.5 %, while both *Aulacoseira* species show a minimum (Fig. 6). *D. stelligera* (basionym *Cyclotella stelligera*; Guiry and Guiry, 2024), belongs to diatoms of the *Cyclotella sensu lato* taxa (Saros and Anderson, 2015). The shift in diatom assemblage characterised by an increase of small cyclotelloid planktonic diatoms like the *Cyclotella stelligera* complex and a simultaneously decrease of *Aulacoseira* taxa and/or small benthic fragilariod taxa is revealed in other paleolimnological studies from the northern hemisphere (Rühland et al., 2003; Smol et al., 2005; Rühland et al., 2008). Diatom zone 5 corresponds with a hydroclimatic phase of the $\delta^{18}O_{diatom}$ record, indicating increased winter precipitation and more snowmelt water supply to Lake Khamra, supported by meteorological data (Fig. 6) (Stieg et al., 2024b). Despite increased water turbulence from inflow, which usually benefits *Aulacoseira*, its observed decrease is unexpected. Therefore, we infer that an additional factor is responsible for the decline. Since the 1970s regional annual temperature start to increase (Anomalies of annual mean temperature, Vitim; Fig. 6). Rising temperatures in the context of global warming, likely reduce the ice–cover duration and increase the possibility of thermal stratification of the lake water in the ice–free period, which allow *D. stelligera* to thrive (Smol et al., 2005; Rühland et al., 2015). Increased summer stratification is less favourable for *Aulacoseira* (Gibson et al., 2003; Rühland et al., 2008), although it remains dominant at Lake Khamra (>50 %, Fig. 3).

Additionally, we observe a rapid increase in the silicified chrysophyte *Mallomonas* scales since the 1990s, inferred from the *Mallomonas* index (M/D) (Fig. 3). Chrysophytes are common in oligotrophic environments (Smol, 1985). Their motility, enabled by flagella, allows them to thrive in stratified lakes by maintaining their position in the photic zone. This gives them an advantage over non-motile, colonial diatoms such as *Aulacoseira* (Ginn et al., 2010; Mushet et al., 2017). The observed increase in chrysophytes at Lake Khamra suggests changes in the lake's mixing regime. Further it provides evidence for a likely longer ice-free period and enhanced thermal stratification during summer months in recent decades. Similar increases in scaled chrysophytes have been reported in other lake systems, associated with climate warming and increased thermal stability (Paterson et al., 2004; Ginn et al., 2010; Favot et al., 2024).

An increase of annual temperature and a shorter lake ice period extend the diatom growing season and change light and nutrient availability, favouring small planktonic diatoms (Rühland et al., 2015). Observed elevated diatom species richness (Hill's N0, Fig. 3) are congruent with reported increased diatom community complexity and diversity during prolonged ice–free periods in Arctic lakes (Douglas and Smol, 2010; Rühland et al., 2015). Different studies have reported a rise in pennate (tychoplanktonic) planktonic *Fragilaria* populations as a response to climate warming (Rühland et al., 2013; Michelutti et al., 2015; Sochuliakova et al., 2018). *S. pinnata* and *F. radians* both group together with *D. stelligera* in the PCA biplot (Fig. 4), and *F. radians* also occur primarily in the uppermost diatom zone (Fig. 2), underlining a possible common reaction to warming at Lake Khamra.

In many Arctic lakes, comparable shifts in the diatom community occurred as early as 1850 CE (Smol et al., 2005), while the change at Lake Khamra occurred about 120 years later. The timing discrepancy regarding the onset of increase in small *Cyclotella sensu lato* species aligns with studied temperate regions in North America and Europe (Rühland et al., 2008), which also show a change from 1970 CE onwards. Yakutian lakes are rare in circumpolar studies (Smol et al., 2005; Rühland et al., 2008). A similar shift in diatom composition has been observed at Lake Bolshoe Toko, a comparable remote boreal lake in eastern Siberia, after 1850 CE, interpreted as a response to

climate warming (Biskaborn et al., 2021b). However, the much lower stratigraphic resolution at Lake Bolshoe Toko introduces age uncertainties, making direct comparison with the Lake Khamra record difficult. The observed age offset in diatom shifts could refer to different climate related drivers. Further diatom assemblage shifts are observed at the south basin of Lake Baikal at ca. 1970 CE (Roberts et al., 2018), as well as at pristine Arctic and sub–Arctic lakes in the northern Urals with most distinct shifts after 1970 CE (Solovieva et al., 2008). Our data align with the later onset of diatom assemblage changes at lower latitudes compared to the earlier changes observed in Arctic regions, which is attributed to an earlier warming and a quicker response of Arctic ecosystems compared to lower latitudes (Smol et al., 2005; Smol and Douglas, 2007).

The shifts in diatom assemblage delineating zones 4 and 5 as well as 1 and 2 have similarities (*Aulacoseira* decline while planktonic cyclotelloid taxa such as *S. alpinus* or *D. stelligera* increase and diatom richness increase). However, we also see clear differences (cold habitat preferences from *S. alpinus* vs. warm and stratified preferences of *D. stelligera*, increase of *F.radians* and *S. pinnata* in recent years only) which suggests that the increase in air temperatures in recent decades notably influenced the lake ecosystem and its diatom assemblages.
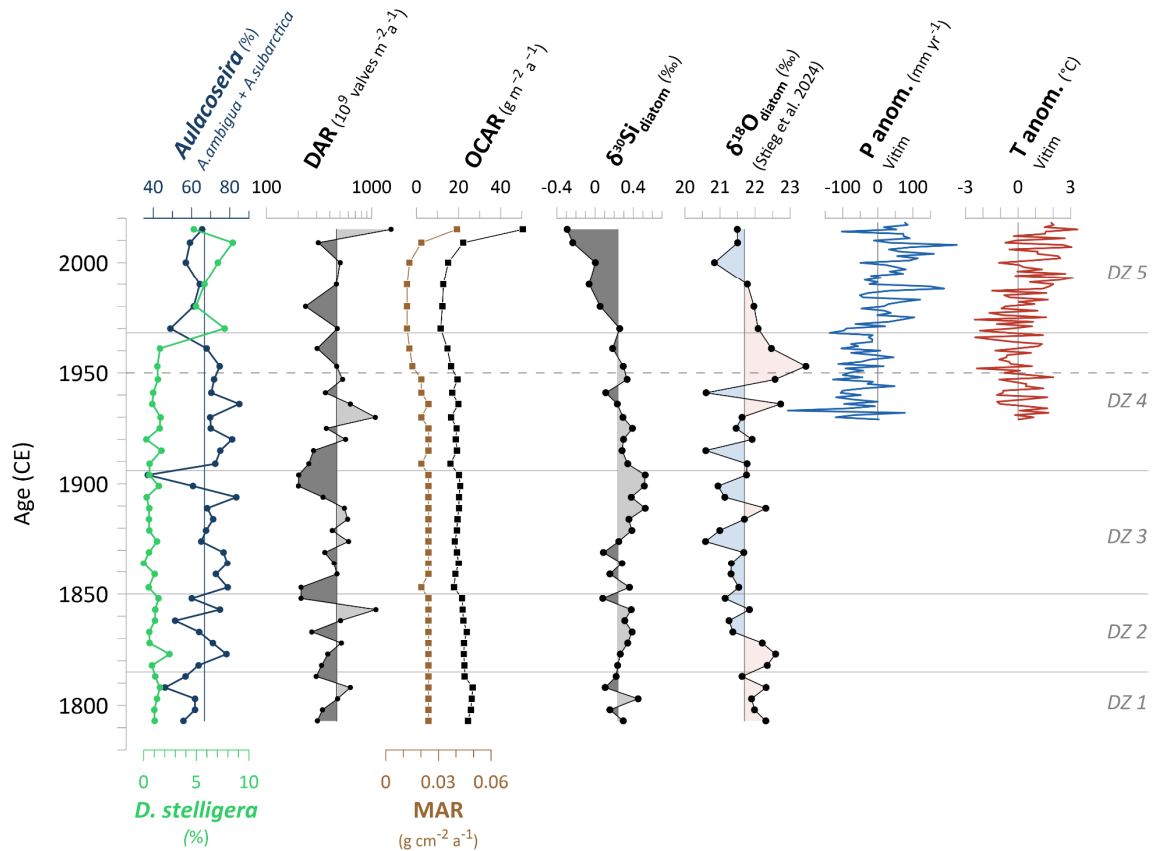
Figure 6. Diatom assemblage changes and selected biogeochemical proxies in relation to hydroclimatic variability: *Aulacoseira* **vs.** *D.stelligera* **abundances of the short core EN18232-1; diatom accumulation rates (DAR); mass accumulation rates (MAR) and carbon accumulation rates (OCAR); δ³⁰Si_diatom record; δ¹⁸O_diatom record from the same short core of Lake Khamra (Stieg et al., 2024b); Anomalies of annual mean temperature and annual precipitation from the weather station in Vitim (59.45° N, 112.58° E; 186 m a.s.l.; ECA (European Climate Assessment); data accessible via the KNMI Climate Explorer https://climexp.knmi.nl; last access: 15. July 2024; (Klein Tank et al., 2002). Vertical lines indicate the individual mean values. Horizontal lines indicate diatom zones (DZ), the dashed line marks the time before and after 1950 CE.**

4.3 Biogeochemical proxies as indicators of bioproductivity and organic matter sources at Lake Khamra

4.3.1 Biogeochemical shifts after ca. 1950 CE

Carbon and nitrogen indicators (TOC, TN, C/N, OCAR, δ^{13}C; Fig. 5) show a notable shift at ~1950 CE, highlighting substantial limnological changes that precede the major shifts in diatom communities observed starting at ca. 1970 CE (onset of diatom zone 5). We propose that hydroclimatic variability substantially influences limnological conditions at Lake Khamra, with some diatom species responding immediately. However, the most ecologically important shift in the diatom assemblage appears to occur ~1970 CE and is more likely driven by rising temperatures and their associated limnological effects, as discussed above.

At ~1950 CE, the $\delta^{18}O_{diatom}$ values reach a maximum (Fig. 6), interpreted as a dry anomaly with reduced input of isotopically light winter precipitation into the lake (Stieg et al., 2024b). This reconstructed anomaly aligns with the overall dry period inferred from persistently below-average annual precipitation starting from the 1930s, at the onset of meteorological recordings, and continuing until the 1970s (Fig. 6; details in Stieg et al., 2024b). Additionally, a charcoal record from the same lake identifies enhanced fire activity during the 1950s (Glückler et al., 2021), coinciding with the $\delta^{18}O_{diatom}$ maximum, providing further evidence of this dry anomaly. At the same time, mass accumulation rates (MARs) drop (Fig. 6), which could be linked to a reduction in erosional input, further supported by the flattening of the age-depth relationship from the 1950s onwards (Fig. A1), indicating lower sedimentation rates. The concurrent decrease in organic carbon accumulation rate (OCAR) to a minimum of 11.5 g m^{-2} a^{-1} between ca. 1950 and 1970 (Fig. 5 & 6) suggests lower erosional input of organic material, a reduced primary productivity, or a combination of both. In addition to the dry phase, declining annual temperatures, reaching a minimum between ~1950 and 1970 CE (Fig. 6), indicate simultaneously cool conditions. While *Aulacoseira* remains dominant, it decreases especially between the 1950s and the 1970s. Diatom accumulation rates (DARs) decline after the peak in the 1930s indicating rather a reduction in primary productivity around the 1950s. This is likely linked to cold annual temperature anomalies and less nutrient refreshment due to reduced turbulence and inflow, as *Aulacoseira* begins to decline. In contrast, total organic carbon (TOC) and total nitrogen (TN), which represent the fraction of organic matter and are closely related to primary productivity (Meyers and Teranes, 2001), both show a peak between ca. 1950 and 1970 CE (Fig. 5), indicating higher bioproductivity. It is plausible, that low sedimentation rates could result in a relative increase in TOC and TN concentrations within the sediment, explaining the contrasting tendency.

During the dry period between the 1950s and 70s, the erosional input from the catchment was probably reduced. However, a differentiation between autochthonous (in–lake) or allochthonous origin of organic material since then remains indistinct. The atomic organic carbon–to–nitrogen ratio (C/N) together with δ^{13}C help to identify the organic matter origin (Meyers, 2009). C/N drops from ca. 13 to a slightly lower level of around 12 since the 1950s, reflecting a mixed signal in both cases. According to the literature, lacustrine algae have a C/N ratio ranging between 4 and 10, whereas organic matter from land plants have a ratio >20 (Meyers and Teranes, 2001). Also together with δ^{13}C, a differentiation still remains inexplicit (Fig. 7), as both, algae and C$_3$–land plants, have similar δ^{13}C signatures, making them indistinguishable (Meyers, 2009). The δ^{15}N data underlines a mixed organic origin, as the value of 3 ‰ lies in between land plants (around 0 ‰) and freshwater algae (5–10 ‰, (Meyers, 2009). However, the rather low C/N values tend towards an autochthonous organic matter source since the 1950s, underlining a reduced inflow from the catchment.

After ~1970 CE, during diatom zone 5, annual precipitation in the region increases (Fig. 6) and offer the possibility for an increased erosional input from the catchment. Simultaneously, we observe an increase in both TOC and TN (Fig. 5), pointing towards a higher bioproductivity (Meyers and Teranes, 2001). Since OCAR increases at the same time (Fig. 5), it supports an enhanced accumulation of TOC from ca. 1970 CE onwards. However, the C/N ratio in combination with $\delta^{13}C$ still mirrors a mixed signal of its origin (Fig. 7). The DAR lags slightly behind and increases after the 1980s (Fig. 6), indicating a tendency towards enhanced diatom productivity likely related to warming (Douglas and Smol, 2010; Biskaborn et al., 2012; Biskaborn et al., 2021b).
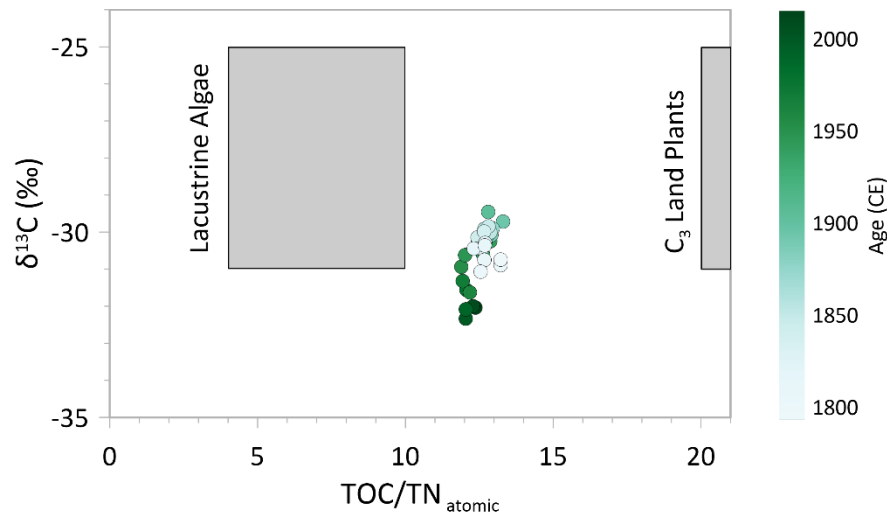
Figure 7. C/N–$\delta^{13}C$–plot showing sediment samples of the short core EN18232-1. In general, lacustrine algae have a C/N ratio between 4 to 10, C₃ land plants have a ratio > 20 (Meyers and Teranes, 2001). Figure is based on the values given by Meyers and Teranes (2001).

The continuous decrease in $\delta^{13}C$ especially since the 1950s (Fig. 5) initially appears to contradict the interpretation of increased bioproductivity in the upper part of the record, even though algae and land plants have similar signatures (Meyers, 2009). In general, phytoplankton preferentially incorporates lighter ^{12}C than ^{13}C, which enriches the remaining reservoir over time and lead to increasing $\delta^{13}C$ values of organic matter during enhanced productivity (Meyers, 2009). The observed $\delta^{13}C$ decline might, at least partly, be related to fossil fuel combustion and biomass burning, which release CO_2 depleted in ^{13}C into the atmosphere, known as *Suess effect* (Keeling, 1979). As the CO_2 in the atmosphere and in the water tend to reach equilibrium, this also effects the $\delta^{13}C$ values of lake sediment organic matter (Verburg, 2007), as observed e.g. in a lake study in West Greenland (Stevenson et al., 2021). Most of the decline in $\delta^{13}C$ of about 1.7 ‰ at Lake Khamra could, thus, be explained by the decline in atmospheric $\delta^{13}C$, which has accelerated particularly after 1950 and has fallen by about 1 ‰ since then (Verburg, 2007). Aside from that, an increased algae productivity might not contradict with decreasing $\delta^{13}C$ values, as light CO_2 can be constantly assimilated during increased growth, as observed in an Arctic lake (Jiang et al., 2011).

As with $\delta^{13}C$, $\delta^{30}Si_{diatom}$ also shows a decline, but slightly later at around 1970 CE (Fig. 5 & 6), coinciding with the shift of the diatom assemblages between diatom zones 4 and 5. We assume that the decrease in $\delta^{30}Si_{diatom}$ is influenced by multiple factors, as the interpretation of silicon isotopes is complex and involves various processes (Sutton et al., 2018). Overall, the $\delta^{30}Si_{diatom}$ values are low (mean: +0.24 ‰), comparable to e.g. a study at a groundwater–dominated Swedish lake (Zahajská et al., 2021a). Groundwater inflow could lead to low isotope

values of dissolved silica (DSi, $\delta^{30}Si_{DSi}$) and hence to low $\delta^{30}Si_{diatom}$ (Opfergelt et al., 2011; Frings et al., 2016; Zahajská et al., 2021b; Zahajská et al., 2021a). Unfortunately, there is no information on lake water $\delta^{30}Si_{DSi}$ or groundwater inflow at Lake Khamra. It is likely that groundwater input at Lake Khamra contributes to the generally low $\delta^{30}Si_{diatom}$. However, a sudden change in groundwater seems unlikely and cannot explain the distinct decrease at around 1970 CE.

Fractionation of silicon isotopes occurs through both inorganic chemical weathering and biological activities, mainly diatom growth in marine and terrestrial environments (Opfergelt et al., 2011). In marine environments, diatom silicon utilisation is linked with the silicon isotope composition (De la Rocha et al., 2000; Varela et al., 2004; Cardinal et al., 2005; De La Rocha, 2006), whereas studies in lacustrine environments are sparse. There are studies linking diatom blooms in lakes with silicon isotope fractionation by seasonal *in situ* measurements to validate $\delta^{30}Si_{diatom}$ as a bioproductivity proxy (Alleman et al., 2005; Opfergelt et al., 2011; Panizzo et al., 2016). In this context, $\delta^{30}Si_{diatom}$ is used as a paleoenvironmental proxy in only few paleolimnology studies in Asia, for example at Lake El'gygytgyn in North East Siberia (Swann et al., 2010), or in South China (Chen et al., 2012). Diatoms preferably incorporate light ^{28}Si instead of heavier ^{30}Si (and ^{29}Si) during biomineralization (De La Rocha et al., 1997; Leng et al., 2009). Assuming this fractionation dominates the isotopic signal of the diatoms at Lake Khamra, the decrease of $\delta^{30}Si_{diatom}$ to values of -0.53 ‰ in recent decades contradicts the discussed tendency towards higher algae productivity in diatom zone 5. Higher bioproductivity increases DSi utilisation and would result in both, an enrichment of the DSi signature of the reservoir (lake water) and of the diatom frustules therein. In unlimited lake systems, such as Lake Khamra, alteration of DSi sources can influence $\delta^{30}Si_{diatom}$ (Zahajská et al., 2021b), and may overprint the isotopic effect of bioproductivity. We suggest that substantial changes in the catchment have led to isotopic changes in the reservoir (lake water), which influenced the $\delta^{30}Si_{diatom}$ record at Lake Khamra. Since ~1970 CE, both temperature and precipitation increase in the region (Fig. 6), forcing enhanced weathering in the catchment and e.g. leading to a higher nutrient inflow to the lake (Douglas and Smol, 2010), as supported by the increase in OCAR (Fig. 5). In addition, the recent wet and warm period at Lake Khamra follows an earlier cold and dry period around the 1950s with increased wildfire activity in the region (Glückler et al., 2021; Stieg et al., 2024b). Fires in the catchment area have likely altered vegetation and soil conditions, consequently affecting the source of dissolved silica. Soils and terrestrial plants, which tend to have low $\delta^{30}Si_{DSi}$ values (Frings et al., 2016; Sun et al., 2018), may be subject to increased erosion following the (partial) loss of the vegetation cover. Additionally, Lake Khamra lies within a sporadic permafrost zone (Fedorov et al., 2018). Observed warming could increase the depth of the active layer, which as it thaws, would also preferably transport low $\delta^{30}Si_{DSi}$ from litter and soil material into the lake.

Besides the change of catchment supply, an alteration of species composition driven by variations in summer temperatures and the duration of ice–free periods (Zahajská et al., 2021b) could further influence $\delta^{30}Si_{diatom}$. It remains uncertain if a species effect leads to a different silicon isotope fractionation. While Sutton et al. (2013) provided evidence of such effects in marine diatoms, Schmidtbauer et al. (2022) observed varying $\delta^{30}Si_{diatom}$ values in lacustrine samples, which were associated with different preferred habitat regimes. We hypothesise, the $\delta^{30}Si_{diatom}$–decrease at Lake Khamra could partially mirror the major shift in diatom assemblage since the 1970s, from heavy and compact *Aulacoseira* taxa to less silicified *D. stelligera*. Overall, interpreting $\delta^{30}Si_{diatom}$ in lacustrine systems is more complex than in marine environments. At Lake Khamra, $\delta^{30}Si_{diatom}$ appears to be influenced by multiple factors, including shifts in diatom assemblages and catchment alterations that affect silica sources and utilisation.

4.3.2 Biogeochemical trends before ca. 1950 CE

Before ~1950 CE we observe a prolonged, rather stable period in most biogeochemical proxies (TOC, TN, C/N, OCAR, $\delta^{13}C$, $\delta^{30}Si_{diatom}$, $\delta^{15}N$; Fig. 5) characterised by a dominance of *Aulacoseira* in diatom zones 2, 3 and 4. The slightly elevated C/N ratio of around 13 in combination with elevated $\delta^{13}C$ values (Fig. 7) still indicate a mixed source signal of organic material, as outlined above. Compared to the period after ~1950 CE, the older section of the record shows a tendency towards a more allochthonous origin of the organic material (Meyers, 2009), which could indicate either lower lake-internal productivity or increased erosional inflow of organic matter. Only a few species dominated the record at this time (lowest Hill's N2; Fig. 3), mainly represented by the two *Aulacoseira* taxa. TOC and TN values show their lowest concentration between ~1830 and 1950 CE (Fig. 5), suggesting a reduced bioproductivity (Meyers and Teranes, 2001). OCAR values are less indicative and remain relatively constant until the 1950s (Fig. 5), with DAR showing similar stability, though with some dips indicating periods of lower accumulation (Fig. 6). These trends point to a relatively constant or slightly decreased bioproductivity. As referred from the $\delta^{18}O_{diatom}$ record (Fig. 6) (Stieg et al., 2024b), the hydroclimatic conditions were rather stable since ~1830 CE, likely with sufficient inflow from the catchment by snowmelt. This rather wet period could explain the tendency towards an allochthonous origin of organic material.

Instead, elevated $\delta^{30}Si_{diatom}$ would suggest enhanced bioproductivity based on the classical interpretation of this proxy (De La Rocha et al., 1997). *Aulacoseira* has a high demand of dissolved silica for their heavy and thick frustules, which could have led to a moderate $\delta^{30}Si$ enrichment of the reservoir during phases of diatom bloom. Furthermore, we assume that, in contrast to the post–1950s period, the catchment was not yet affected by wildfire disturbances, leading to a difference in the isotopic signature of pre and post 1950s. Less influence of isotopic light $\delta^{30}Si$ plant material from soil erosion potentially resulted in a higher $\delta^{30}Si$ level of dissolved silica, which is reflected in the overall elevated $\delta^{30}Si_{diatom}$ (Fig. 6). This highlights the complexity of $\delta^{30}Si_{diatom}$ as a proxy, linked likely to both in-lake biogeochemical processes and catchment dynamics at Lake Khamra.

4.4 Anthropogenic influence on Lake Khamra linked to atmospheric pollution

There are indications of human pollution at Lake Khamra, despite its remote location and the absence of industrial activity in its vicinity. The decline in $\delta^{13}C$ values since the 1950s (Fig. 5) is likely linked to the release of lighter carbon isotopes from fossil fuel combustion (Verburg, 2007), as reflected in the lake's sediments.

A previous study (Stieg et al., 2024b) identified a marked increase in mercury concentrations in the same lake sediment samples, tripling since ~1930 CE, with fluxes rising more than fourfold since the 1990s. Mercury in the lake can originate from both natural sources, such as permafrost (Rutkowski et al., 2021), and biomass burning (Burke et al., 2010; Driscoll et al., 2013), as well as from anthropogenic sources, such as emissions (Wang et al., 2004; Streets et al., 2011). The observed increase at Lake Khamra is at least partly related to industrial growth and associated atmospheric mercury emissions in Asia and Russia (Pacyna et al., 2016; Sundseth et al., 2017; Eckhardt et al., 2023), comparable to mercury accumulation rates observed at Lake Baikal post-1850 CE (Roberts et al., 2020). Here, atmospheric fallout since the 1980s is also suggested to have likely contributed to rising mercury accumulation rates, in addition to mining activities in the vicinity of Lake Baikal (Roberts et al., 2020). Similarly, a rapid mercury increase since 1850 CE has been linked to atmospheric pollution at another remote boreal lake in

eastern Siberia (Biskaborn et al., 2021b), suggesting that Lake Khamra is likely also influenced by anthropogenic mercury deposition.

In contrast to the recent marked increase in mercury levels and $\delta^{13}C$ depletion, $\delta^{15}N$ in Lake Khamra sediments has shown only minimal variation over the last ~220 years, fluctuating by ±0.5‰, with a slight decrease of ~0.3‰ since the 1970s (Fig. 5). Human activities, such as fossil fuel combustion and fertilizer production, are relevant sources of reactive nitrogen (Nr) that contribute to the deposition of $\delta^{15}N$-depleted nitrogen in lake sediments, typically in a range from 1–3‰ (Gruber and Galloway, 2008; Holtgrieve et al., 2011; Wolfe et al., 2013). Despite the possible influence of atmospheric pollution, no substantial $\delta^{15}N$ depletion is observed in Lake Khamra. However, not all lakes display $\delta^{15}N$ depletion, as nitrogen cycling in lakes is complex, and factors such as nitrogen inputs, water residence time, and aquatic activity play crucial roles (Meyers and Teranes, 2001; Galloway et al., 2003; Anderson et al., 2018). For example, increased abundance of *A. formosa* in oligotrophic alpine lakes in North America has been linked to atmospheric nitrogen deposition (Saros et al., 2005; Saros et al., 2010). At Lake Khamra, we observe only a slight increase in planktonic *A. formosa* in the most recent diatom zone 5 (Fig. 2). We suggest that this slight increase in abundance is more likely a response to climate warming and related changes in like water mixing and thermal stability rather than nitrogen enrichment by atmospheric deposition (Sivarajah et al., 2016). This further supports the argument that Lake Khamra is primarily influenced by recent climate warming, which is altering the lake's properties, rather than by atmospheric nitrogen deposition from human sources.

5   Conclusions

Our study of diatom assemblages and biogeochemical proxies over the last ~220 years from Lake Khamra, eastern Siberia, reveals distinct ecosystem changes, likely driven by hydroclimatic dynamics. This research addresses a spatial gap in lake studies over shorter time periods in Yakutia.

Lake Khamra's diatom assemblage is dominated by planktonic diatom species, primarily *Aulacoseira* taxa. At ca. 1970 CE, we observe a major shift in the diatom assemblages, characterised mainly by an increase in planktonic *D. stelligera*, while the two dominant *Aulacoseira* taxa decrease. We attribute this change to warming, a probable earlier ice–out, and a potential increase in summer thermal stratification in the recent decades. Rapidly increasing chrysophyte scales (*Mallomonas*) since the 1990s support the warming trend and a related increasing stratification of the lake. These findings are temporally consistent with similar changes observed in temperate lake ecosystems globally.

Carbon and nitrogen proxies exhibit changes starting in the 1950s, indicating hydroclimatic influence with a delayed shift in the diatom assemblages, which we attribute primarily to rising temperatures and associated effects. At Lake Khamra, the interpretation of $\delta^{30}Si_{diatom}$ is not straightforward, as it is likely influenced by a combination of factors, including weathering, shifts in diatom assemblages, and diatom productivity. We suggest that wildfire activity in the catchment in the 1950s, along with increased precipitation and temperatures since ~1970 CE, altered silica sources by transporting isotopically light dissolved silica into the lake, which likely led to the observed decrease. Furthermore, the lower silica uptake of *D. stelligera* compared to *Aulacoseira* taxa might have further influenced this decline.

In addition to elevated mercury levels determined in a previous study, human influence on Lake Khamra is evident from $\delta^{13}C$ depletion, likely derived from fossil fuel combustion. No substantial $\delta^{15}N$-depletion from atmospheric nitrogen deposition is observed in Lake Khamra sediments.

These findings underline the effects of both climate warming and anthropogenic air pollution on remote lake ecosystems, emphasising the need for comprehensive research to mitigate these impacts and protect natural water resources.

Appendix A

730
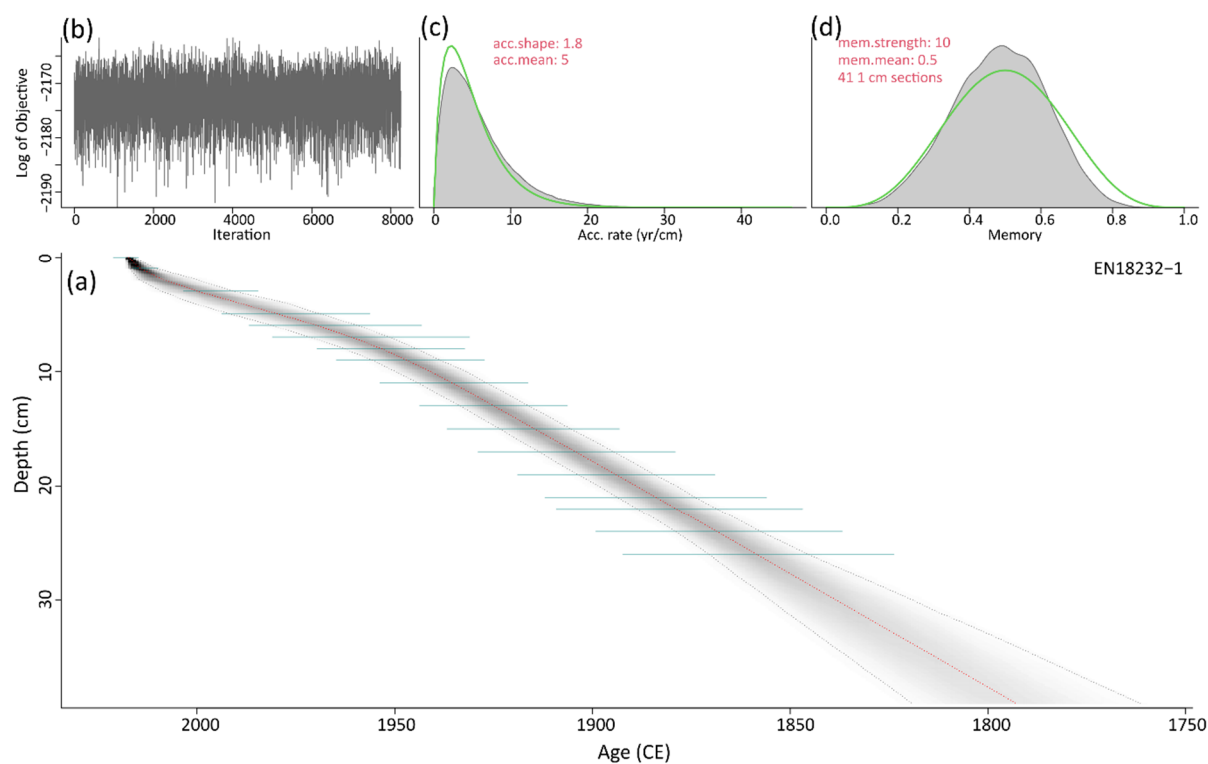
Figure A1. (a) Bayesian accumulation model based on the ^{210}Pb and ^{137}Cs dating (green lines) of the short core EN18232-1 (grey lines indicate the 2σ range; red line indicates the median). (b) Model iteration log. (c, d) Prior (green line) and posterior (grey area) distributions for accumulation rate and memory, respectively. Age–depth model was first published in Stieg et al. (2024b).

735

Data availability.

Datasets used in this study are accessible via PANGAEA, including:

1. Diatom assemblage of the sediment short core EN18232-1 and corresponding indices, https://doi.org/10.1594/PANGAEA.971296, Stieg et al. (dataset in review)

740

2. Diatom silicon isotope record of the sediment short core EN18232-1, https://doi.org/10.1594/PANGAEA.971278, Stieg et al. (dataset in review)

3. Biogeochemical proxies of the sediment short core EN18232-1, https://doi.org/10.1594/PANGAEA.971277, Stieg et al. (dataset in review)

745 **Author contributions.**

AS, HM, BKB and UH conceived the study. UH, BKB and LP conducted fieldwork in 2018 and 2020 and received the sediment core. AS processed and analysed the sediment samples in the lab. AS performed diatom analysis and counting, as well as statistical analysis, under the guidance of BKB. AM measured the silicon isotope samples in BHV, with the support of DWD, and helped together with HM to interpret the diatom isotopes. JS supervised the

750 carbon and nitrogen measurements and helped to interpret the proxies. AS produced all figures and tables and wrote the manuscript. All authors commented on previous versions of the text and approved the final manuscript.

Competing interests. The authors declare that they have no conflict of interest.

755 **Disclaimer.** Colours from the scientific color maps from Crameri et al. (2020) have been used in the figures. Maps throughout this article were created using the Free and Open Source QGIS Geographic Information System. QGIS.org, Version 3.12, 2024.

Acknowledgements. We thank the working groups of the ISOLAB Facility and the CarLa lab of the AWI in

760 Potsdam, as well as the Stable Isotope Facility of the AWI in Bremerhaven. We would further like to thank all participants of the joint German–Russian expedition in Yakutia 2018 and 2020 for their fieldwork. Many thanks to the editor Cindy De Jonge, referee Anson Mackay, and an anonymous reviewer for their valuable and constructive feedback.

765 **Financial support.** AS is funded by AWI INSPIRES (International Science Program for Integrative Research in Earth Systems).

References

Alleman, L. Y., Cardinal, D., Cocquyt, C., Plisnier, P.-D., Descy, J.-P., Kimirei, I., Sinyinza, D., and André, L.: Silicon Isotopic Fractionation in Lake Tanganyika and Its Main Tributaries, Journal of Great Lakes Research, 31, 509-519, https://doi.org/10.1016/S0380-1330(05)70280-X, 2005.

AMAP: AMAP Arctic Climate Change Update 2021: Key Trends and Impacts. Arctic Monitoring and Assessment Programme (AMAP), Tromsø, Norway, viii+148pp, 978-82-7971-201-5, 2021.

Anderson, N. J., Curtis, C. J., Whiteford, E. J., Jones, V. J., McGowan, S., Simpson, G. L., and Kaiser, J.: Regional variability in the atmospheric nitrogen deposition signal and its transfer to the sediment record in Greenland lakes, Limnology and Oceanography, 63, 2250-2265, 10.1002/lno.10936, 2018.

Appleby, P. G., Nolan, P. J., Gifford, D. W., Godfrey, M. J., Oldfield, F., Anderson, N. J., and Battarbee, R. W.: 210Pb dating by low background gamma counting, Hydrobiologia, 143, 21-27, 10.1007/bf00026640, 1986.

Bahls, L. L.: The role of amateurs in modern diatom research, Diatom Research, 30, 209-210, 10.1080/0269249X.2014.988293, 2015.

Barinova, S., Nevo, E., and Bragina, T.: Ecological assessment of wetland ecosystems of northern Kazakhstan on the basis of hydrochemistry and algal biodiversity, Acta Botanica Croatica, 70, 215-244, 10.2478/v10184-010-0020-7, 2011.

Battarbee, R. W. and Kneen, M. J.: The use of electronically counted microspheres in absolute diatom analysis, Limnology and Oceanography, 27, 184-188, 10.4319/lo.1982.27.1.0184, 1982.

Battarbee, R. W., Jones, V. J., Flower, R. J., Cameron, N. G., Bennion, H., Carvalho, L., and Juggins, S.: Diatoms, in: Tracking Environmental Change Using Lake Sediments: Terrestrial, Algal, and Siliceous Indicators, edited by: Smol, J. P., Birks, H. J. B., Last, W. M., Bradley, R. S., and Alverson, K., Springer Netherlands, Dordrecht, 155-202, 10.1007/0-306-47668-1_8, 978-0-306-47668-6, 2001.

Birks, H. J. B.: Numerical methods for the analysis of diatom assemblage data, in: The Diatoms: Applications for the Environmental and Earth Science, edited by: Smol, J. P., and Stoermer, E. F., Cambridge University Press, Cambridge, 23–54, https://doi.org/10.1017/CBO9780511763175, 2010.

Biskaborn, B. K., Herzschuh, U., Bolshiyanov, D., Savelieva, L., and Diekmann, B.: Environmental variability in northeastern Siberia during the last ~ 13,300 yr inferred from lake diatoms and sediment–geochemical parameters, Palaeogeography, Palaeoclimatology, Palaeoecology, 329-330, 22-36, 10.1016/j.palaeo.2012.02.003, 2012.

Biskaborn, B. K., Bolshiyanov, D., Grigoriev, M. N., Morgenstern, A., Pestryakova, L. A., Tsibizov, L., and Dill, A.: Russian-German Cooperation: Expeditions to Siberia in 2020 , Berichte zur Polar- und Meeresforschung = Reports on polar and marine research, Alfred Wegener Institute for Polar and Marine Research, Bremerhaven, 81, 10.48433/BzPM_0756_2021, 2021a.

Biskaborn, B. K., Narancic, B., Stoof-Leichsenring, K. R., Pestryakova, L. A., Appleby, P. G., Piliposian, G. T., and Diekmann, B.: Effects of climate change and industrialization on Lake Bolshoe Toko, eastern Siberia, Journal of Paleolimnology, 65, 335-352, 10.1007/s10933-021-00175-z, 2021b.

Biskaborn, B. K., Forster, A., Pfalz, G., Pestryakova, L. A., Stoof-Leichsenring, K., Strauss, J., Kröger, T., and Herzschuh, U.: Diatom responses and geochemical feedbacks to environmental changes at Lake Rauchuagytgyn (Far East Russian Arctic), Biogeosciences, 20, 1691-1712, 10.5194/bg-20-1691-2023, 2023.

Biskaborn, B. K., Nazarova, L., Kröger, T., Pestryakova, L. A., Syrykh, L., Pfalz, G., Herzschuh, U., and Diekmann, B.: Late Quaternary Climate Reconstruction and Lead-Lag Relationships of Biotic and Sediment-Geochemical Indicators at Lake Bolshoe Toko, Siberia, Frontiers in Earth Science, 9, 737353, 10.3389/feart.2021.737353, 2021c.

Biskaborn, B. K., Subetto, D. A., Savelieva, L. A., Vakhrameeva, P. S., Hansche, A., Herzschuh, U., Klemm, J., Heinecke, L., Pestryakova, L. A., Meyer, H., Kuhn, G., and Diekmann, B.: Late Quaternary vegetation and lake system dynamics in north-eastern Siberia: Implications for seasonal climate variability, Quaternary Science Reviews, 147, 406-421, 10.1016/j.quascirev.2015.08.014, 2016.

Blaauw, M. and Christen, J. A.: Flexible paleoclimate age-depth models using an autoregressive gamma process, Bayesian Analysis, 6, 457-474, 10.1214/11-ba618, 2011.

Burke, M. P., Hogue, T. S., Ferreira, M., Mendez, C. B., Navarro, B., Lopez, S., and Jay, J. A.: The Effect
of Wildfire on Soil Mercury Concentrations in Southern California Watersheds, Water Air Soil Pollut,
212, 369-385, 10.1007/s11270-010-0351-y, 2010.

Cardinal, D., Alleman, L. Y., Dehairs, F., Savoye, N., Trull, T. W., and André, L.: Relevance of silicon
isotopes to Si-nutrient utilization and Si-source assessment in Antarctic waters, Global Biogeochemical
Cycles, 19, GB2007, 10.1029/2004gb002364, 2005.

Chapligin, B., Meyer, H., Friedrichsen, H., Marent, A., Sohns, E., and Hubberten, H. W.: A high-
performance, safer and semi-automated approach for the δ18O analysis of diatom silica and new
methods for removing exchangeable oxygen, Rapid Commun Mass Spectrom, 24, 2655-2664,
10.1002/rcm.4689, 2010.

Chelnokova, S. M., Chikina, I. D., and Radchenko, S. A. Geologic map of Yakutia P-48,49, 1 : 1000000,
VSEGEI, Leningrad: http://www.geokniga.org/sites/geokniga/, last access: 11. November 2022.

Chen, J., Li, J., Tian, S., Kalugin, I., Darin, A., and Xu, S.: Silicon isotope composition of diatoms as a
paleoenvironmental proxy in Lake Huguangyan, South China, Journal of Asian Earth Sciences, 45, 268-
274, 10.1016/j.jseaes.2011.11.010, 2012.

Cherapanova, M. V., Snyder, J. A., and Brigham-Grette, J.: Diatom stratigraphy of the last 250 ka at
Lake El'gygytgyn, northeast Siberia, Journal of Paleolimnology, 37, 155-162, 10.1007/s10933-006-
9019-4, 2006.

Clayton, R. N. and Mayeda, T. K.: The use of bromine pentafluoride in the extraction of oxygen from
oxides and silicates for isotopic analysis, Geochim Cosmochim Ac, 27, 43-52, 10.1016/0016-
7037(63)90071-1, 1963.

Crameri, F., Shephard, G. E., and Heron, P. J.: The misuse of colour in science communication, Nat
Commun, 11, 5444, 10.1038/s41467-020-19160-7, 2020.

Crutzen, P. J. and Stoermer, E. F.: The "Anthropocene", Global Change Newsletters, 41, 17-18, 0284-
5865, 2000.

De La Rocha, C. L.: Opal-based isotopic proxies of paleoenvironmental conditions, Global
Biogeochemical Cycles, 20, GB4S09, 10.1029/2005gb002664, 2006.

De La Rocha, C. L., Brzezinski, M. A., and DeNiro, M. J.: Fractionation of silicon isotopes by marine
diatoms during biogenic silica formation, Geochim Cosmochim Ac, 61, 5051-5056, Doi 10.1016/S0016-
7037(97)00300-1, 1997.

De la Rocha, C. L., Brzezinski, M. A., and DeNiro, M. J.: A first look at the distribution of the stable
isotopes of silicon in natural waters, Geochim Cosmochim Ac, 64, 2467-2477, 10.1016/S0016-
7037(00)00373-2, 2000.

De La Rocha, C. L., Brzezinski, M. A., DeNiro, M. J., and Shemesh, A.: Silicon-isotope composition of
diatoms as an indicator of past oceanic change, Nature, 395, 680-683, Doi 10.1038/27174, 1998.

Dixon, W. J.: Processing Data for Outliers, Biometrics, 9, 74 - 89, 10.2307/3001634, 1953.

Douglas, M. S. V. and Smol, J. P.: Freshwater diatoms as indicators of environmental change in the High
Arctic, in: The diatoms: applications for the environmental and earth sciences, edited by: Smol, J. P.,
and Stoermer, E. F., Cambridge University Press, Cambridge, 249-266, 9780521509961, 2010.

Driscoll, C. T., Mason, R. P., Chan, H. M., Jacob, D. J., and Pirrone, N.: Mercury as a Global Pollutant:
Sources, Pathways, and Effects, Environmental Science & Technology, 47, 4967-4983,
10.1021/es305071v, 2013.

Eckhardt, S., Pisso, I., Evangeliou, N., Zwaaftink, C. G., Plach, A., McConnell, J. R., Sigl, M., Ruppel, M.,
Zdanowicz, C., Lim, S., Chellman, N., Opel, T., Meyer, H., Steffensen, J. P., Schwikowski, M., and Stohl,
A.: Revised historical Northern Hemisphere black carbon emissions based on inverse modeling of ice
core records, Nat Commun, 14, 271, 10.1038/s41467-022-35660-0, 2023.

Favot, E. J., Rühland, K. M., Paterson, A. M., and Smol, J. P.: Sediment records from Lake Nipissing (ON,
Canada) register a lake-wide multi-trophic response to climate change and reveal its possible role for
increased cyanobacterial blooms, Journal of Great Lakes Research, 50, 10.1016/j.jglr.2023.102268,
2024.

Fedorov, A., Vasilyev, N., Torgovkin, Y., Shestakova, A., Varlamov, S., Zheleznyak, M., Shepelev, V.,
Konstantinov, P., Kalinicheva, S., Basharin, N., Makarov, V., Ugarov, I., Efremov, P., Argunov, R.,

Egorova, L., Samsonova, V., Shepelev, A., Vasiliev, A., Ivanova, R., Galanin, A., Lytkin, V., Kuzmin, G., and Kunitsky, V.: Permafrost-Landscape Map of the Republic of Sakha (Yakutia) on a Scale 1:1,500,000, Geosciences, 8, 465 - 481, 10.3390/geosciences8120465, 2018.

Firsova, A. D., Chebykin, E. P., Kopyrina, L. I., Rodionova, E. V., Chensky, D. A., Gubin, N. A., Panov, V. S., Pogodaeva, T. V., Bukin, Y. S., Suturin, A. N., and Likhoshway, Y. V.: Post-glacial diatom and geochemical records of ecological status and water level changes of Lake Vorota, Western Beringia, Journal of Paleolimnology, 66, 407-437, 10.1007/s10933-021-00214-9, 2021.

Frings, P. J., Panizzo, V. N., Sutton, J. N., and Ehlert, C.: Diatom silicon isotope ratios in Quaternary research: Where do we stand?, Quaternary Science Reviews, 344, 10.1016/j.quascirev.2024.108966, 2024.

Frings, P. J., Clymans, W., Fontorbe, G., De La Rocha, C. L., and Conley, D. J.: The continental Si cycle and its impact on the ocean Si isotope budget, Chemical Geology, 425, 12-36, 10.1016/j.chemgeo.2016.01.020, 2016.

Galloway, J. N., Aber, J. D., Erisman, J. W., Seitzinger, S. P., Howarth, R. W., Cowling, E. B., and Cosby, B. J.: The nitrogen cascade, Bioscience, 53, 341-356, Doi 10.1641/0006-3568(2003)053[0341:Tnc]2.0.Co;2, 2003.

Geng, R., Andreev, A., Kruse, S., Heim, B., van Geffen, F., Pestryakova, L., Zakharov, E., Troeva, E., Shevtsova, I., Li, F., Zhao, Y., and Herzschuh, U.: Modern Pollen Assemblages From Lake Sediments and Soil in East Siberia and Relative Pollen Productivity Estimates for Major Taxa, Frontiers in Ecology and Evolution, 10, 837857, 10.3389/fevo.2022.837857, 2022.

Gibson, C. E., Anderson, N. J., and Haworth, E. Y.: Aulacoseira subarctica: taxonomy, physiology, ecology and palaeoecology, European Journal of Phycology, 38, 83-101, 10.1080/0967026031000094102, 2003.

Ginn, B. K., Rate, M., Cumming, B. F., and Smol, J. P.: Ecological distribution of scaled-chrysophyte assemblages from the sediments of 54 lakes in Nova Scotia and southern New Brunswick, Canada, Journal of Paleolimnology, 43, 293-308, 10.1007/s10933-009-9332-9, 2010.

Glückler, R., Herzschuh, U., Kruse, S., Andreev, A., Vyse, S. A., Winkler, B., Biskaborn, B. K., Pestryakova, L., and Dietze, E.: Wildfire history of the boreal forest of south-western Yakutia (Siberia) over the last two millennia documented by a lake-sediment charcoal record, Biogeosciences, 18, 4185-4209, 10.5194/bg-18-4185-2021, 2021.

Gorokhov, A. N. and Fedorov, A. N.: Current Trends in Climate Change in Yakutia, Geography and Natural Resources, 39, 153-161, 10.1134/s1875372818020087, 2018.

Grimm, E. C.: Coniss - a Fortran-77 Program for Stratigraphically Constrained Cluster-Analysis by the Method of Incremental Sum of Squares, Comput Geosci, 13, 13-35, 10.1016/0098-3004(87)90022-7, 1987.

Gruber, N. and Galloway, J. N.: An Earth-system perspective of the global nitrogen cycle, Nature, 451, 293-296, 10.1038/nature06592, 2008.

Guiry, M. D. and Guiry, G. M. AlgaeBase. World-wide electronic publication, National University of Ireland, Galway.: https://www.algaebase.org, last access: 1. August 2024.

Häkansson, H. and Kling, H.: A light and electron microscope study of previously described and new Stephanodiscus species (bacillariophyceae) from central and northern Canadian lakes, with ecological notes on the species, Diatom Research, 4, 269-288, 10.1080/0269249X.1989.9705076, 1989.

Hampton, S. E., Gray, D. K., Izmest'eva, L. R., Moore, M. V., and Ozersky, T.: The rise and fall of plankton: long-term changes in the vertical distribution of algae and grazers in Lake Baikal, Siberia, PLoS One, 9, e88920, 10.1371/journal.pone.0088920, 2014.

Hampton, S. E., Izmest'Eva, L. R., Moore, M. V., Katz, S. L., Dennis, B., and Silow, E. A.: Sixty years of environmental change in the world's largest freshwater lake – Lake Baikal, Siberia, Global Change Biology, 14, 1947-1958, 10.1111/j.1365-2486.2008.01616.x, 2008.

Hampton, S. E., McGowan, S., Ozersky, T., Virdis, S. G. P., Vu, T. T., Spanbauer, T. L., Kraemer, B. M., Swann, G., Mackay, A. W., Powers, S. M., Meyer, M. F., Labou, S. G., O'Reilly, C. M., DiCarlo, M., Galloway, A. W. E., and Fritz, S. C.: Recent ecological change in ancient lakes, Limnology and Oceanography, 63, 2277-2304, 10.1002/lno.10938, 2018.

Hampton, S. E., Galloway, A. W., Powers, S. M., Ozersky, T., Woo, K. H., Batt, R. D., Labou, S. G., O'Reilly, C. M., Sharma, S., Lottig, N. R., Stanley, E. H., North, R. L., Stockwell, J. D., Adrian, R., Weyhenmeyer, G. A., Arvola, L., Baulch, H. M., Bertani, I., Bowman, L. L., Jr., Carey, C. C., Catalan, J., Colom-Montero, W., Domine, L. M., Felip, M., Granados, I., Gries, C., Grossart, H. P., Haberman, J., Haldna, M., Hayden, B., Higgins, S. N., Jolley, J. C., Kahilainen, K. K., Kaup, E., Kehoe, M. J., MacIntyre, S., Mackay, A. W., Mariash, H. L., McKay, R. M., Nixdorf, B., Noges, P., Noges, T., Palmer, M., Pierson, D. C., Post, D. M., Pruett, M. J., Rautio, M., Read, J. S., Roberts, S. L., Rucker, J., Sadro, S., Silow, E. A., Smith, D. E., Sterner, R. W., Swann, G. E., Timofeyev, M. A., Toro, M., Twiss, M. R., Vogt, R. J., Watson, S. B., Whiteford, E. J., and Xenopoulos, M. A.: Ecology under lake ice, Ecol Lett, 20, 98-111, 10.1111/ele.12699, 2017.

Hofmann, G., Lange-Bertalot, H., and Werum, M.: Diatomeen im Süßwasser-Benthos von Mitteleuropa: Bestimmungsflora Kieselalgen für die ökologische Praxis; über 700 der häufigsten Arten und ihre Ökologie, A.R.G. Gantner Verlag K.G., 908 pp., 9783906166926, 2011.

Holtgrieve, G. W., Schindler, D. E., Hobbs, W. O., Leavitt, P. R., Ward, E. J., Bunting, L., Chen, G., Finney, B. P., Gregory-Eaves, I., Holmgren, S., Lisac, M. J., Lisi, P. J., Nydick, K., Rogers, L. A., Saros, J. E., Selbie, D. T., Shapley, M. D., Walsh, P. B., and Wolfe, A. P.: A coherent signature of anthropogenic nitrogen deposition to remote watersheds of the Northern Hemisphere, Science, 334, 1545-1548, 10.1126/science.1212267, 2011.

Horn, H., Paul, L., Horn, W., and Petzoldt, T.: Long-term trends in the diatom composition of the spring bloom of a German reservoir: is Aulacoseira subarctica favoured by warm winters?, Freshwater Biology, 56, 2483-2499, 10.1111/j.1365-2427.2011.02674.x, 2011.

Huang, S., Zhang, K., Lin, Q., Liu, J., and Shen, J.: Abrupt ecological shifts of lakes during the Anthropocene, Earth-Science Reviews, 227, 103981, 10.1016/j.earscirev.2022.103981, 2022.

ICS, I. C. o. S. International Commission on Stratigraphy. Subcommission on Quaternary Stratigraphy. Working Group on the 'Anthropocene': https://quaternary.stratigraphy.org/working-groups/anthropocene, last access: 18. November 2024.

Izmest'eva, L. R., Moore, M. V., Hampton, S. E., Ferwerda, C. J., Gray, D. K., Woo, K. H., Pislegina, H. V., Krashchuk, L. S., Shimaraeva, S. V., and Silow, E. A.: Lake-wide physical and biological trends associated with warming in Lake Baikal, Journal of Great Lakes Research, 42, 6-17, 10.1016/j.jglr.2015.11.006, 2016.

Jiang, S., Liu, X., Sun, J., Yuan, L., Sun, L., and Wang, Y.: A multi-proxy sediment record of late Holocene and recent climate change from a lake near Ny-Ålesund, Svalbard, Boreas, 40, 468-480, 10.1111/j.1502-3885.2010.00198.x, 2011.

Jones, V. J., Rose, N. L., Self, A. E., Solovieva, N., and Yang, H.: Evidence of global pollution and recent environmental change in Kamchatka, Russia, Global and Planetary Change, 134, 82-90, 10.1016/j.gloplacha.2015.02.005, 2015.

Juggins, S. Juggins, S.: Rioja: Analysis of Quaternary Science Data, R package: https://cran.r-project.org/package=rioja, last access: 25. February 2024.

Kahlert, M., Rühland, K. M., Lavoie, I., Keck, F., Saulnier-Talbot, E., Bogan, D., Brua, R. B., Campeau, S., Christoffersen, K. S., Culp, J. M., Karjalainen, S. M., Lento, J., Schneider, S. C., Shaftel, R., and Smol, J. P.: Biodiversity patterns of Arctic diatom assemblages in lakes and streams: Current reference conditions and historical context for biomonitoring, Freshwater Biology, 67, 116-140, 10.1111/fwb.13490, 2020.

Keeling, C. D.: The Suess effect: 13Carbon-14Carbon interrelations, Environment International, 2, 229-300, 10.1016/0160-4120(79)90005-9, 1979.

Kilham, P., Kilham, S. S., and Hecky, R. E.: Hypothesized resource relationships among African planktonic diatoms, Limnology and Oceanography, 31, 1169-1181, 10.4319/lo.1986.31.6.1169, 1986.

Kilham, S. S., Theriot, E. C., and Fritz, S. C.: Linking planktonic diatoms and climate change in the large lakes of the Yellowstone ecosystem using resource theory, Limnology and Oceanography, 41, 1052-1062, DOI 10.4319/lo.1996.41.5.1052, 1996.

Kirillina, K., Shvetsov, E. G., Protopopova, V. V., Thiesmeyer, L., and Yan, W.: Consideration of anthropogenic factors in boreal forest fire regime changes during rapid socio-economic development:

case study of forestry districts with increasing burnt area in the Sakha Republic, Russia, Environmental Research Letters, 15, 035009, 10.1088/1748-9326/ab6c6e, 2020.

Klein Tank, A. M. G., Wijngaard, J. B., Können, G. P., Böhm, R., Demarée, G., Gocheva, A., Mileta, M., Pashiardis, S., Hejkrlik, L., Kern-Hansen, C., Heino, R., Bessemoulin, P., Müller-Westermeier, G., Tzanakou, M., Szalai, S., Pálsdóttir, T., Fitzgerald, D., Rubin, S., Capaldo, M., Maugeri, M., Leitass, A., Bukantis, A., Aberfeld, R., van Engelen, A. F. V., Forland, E., Mietus, M., Coelho, F., Mares, C., Razuvaev, V., Nieplova, E., Cegnar, T., Antonio López, J., Dahlström, B., Moberg, A., Kirchhofer, W., Ceylan, A., Pachaliuk, O., Alexander, L. V., and Petrovic, P.: Daily dataset of 20th-century surface air temperature and precipitation series for the European Climate Assessment, International Journal of Climatology, 22, 1441-1453, 10.1002/joc.773, 2002.

Komarenko, L. E. and Vasilyeva, I. I.: Presnovodny diatomovye i senezelenye vodorosli vodoemov Yakutii. [Freshwater diatoms and blue-green algae of water bodies of Yakutia][in Russian] , 96 figs., Moscow: Akad. Nauk SSSR, Sibirskoe Otdel., Yakutskii Filial, Inst. Biol., Izdatel. Nauka., [1]-423 pp., 1975.

Kostrova, S. S., Biskaborn, B. K., Pestryakova, L. A., Fernandoy, F., Lenz, M. M., and Meyer, H.: Climate and environmental changes of the Lateglacial transition and Holocene in northeastern Siberia: Evidence from diatom oxygen isotopes and assemblage composition at Lake Emanda, Quaternary Science Reviews, 259, 106905, 10.1016/j.quascirev.2021.106905, 2021.

Krammer, K. and Lange-Bertalot, H.: Bacillariophyceae, 4. Teil: Achnanthaceae, Kritische Ergänzungen zu Navicula (Lineolatae) und Gomphonema, Gesamtliteraturverzeichnis Teil 1 - 4, Süßwasserflora von Mitteleuropa, Band 2/4, Gustav Fischer Verlag, Stuttgart, Jena, 3437306642, 1991.

Krammer, K. and Lange-Bertalot, H.: Bacillariophyceae, 1. Teil: Naviculaceae, Süßwasserflora von Mitteleuropa, Band 2/1, Gustav Fischer Verlag, Jena, 3437353969, 1997a.

Krammer, K. and Lange-Bertalot, H.: Bacillariophyceae, 2. Teil: Bacillariaceae, Epithemiaceae, Surirellaceae, Süßwasserflora von Mitteleuropa, Band 2/2, Gustav Fischer Verlag, Jena, 3437353888, 1997b.

Krammer, K., Lange-Bertalot, H., Håkansson, H., and Nörpel, M.: Bacillariophyceae, 3. Teil: Centrales, Fragilariaceae, Eunotiaceae, Süßwasserflora von Mitteleuropa, Band 2/3, Gustav Fischer Verlag, Stuttgart, Jena, 3437305417, 1991.

Kruse, S., Bolshiyanov, D., Grigoriev, M. N., Morgenstern, A., Pestryakova, L., Tsibizov, L., and Udke, A.: Russian-German Cooperation: Expeditions to Siberia in 2018, Alfred Wegener Institute for Polar and Marine Research, Bremerhaven, 263, https://doi.org/10.2312/BzPM_0734_2019, 2019.

Laing, T. E. and Smol, J. P.: Late Holocene environmental changes inferred from diatoms in a lake on the western Taimyr Peninsula, northern Russia, Journal of Paleolimnology, 30, 231-247, 0.1023/A:1025561905506, 2003.

Leng, M. J. and Barker, P. A.: A review of the oxygen isotope composition of lacustrine diatom silica for palaeoclimate reconstruction, Earth-Science Reviews, 75, 5-27, 10.1016/j.earscirev.2005.10.001, 2006.

Leng, M. J. and Sloane, H. J.: Combined oxygen and silicon isotope analysis of biogenic silica, Journal of Quaternary Science, 23, 313-319, 10.1002/jqs.1177, 2008.

Leng, M. J., Swann, G. E. A., Hodson, M. J., Tyler, J. J., Patwardhan, S. V., and Sloane, H. J.: The Potential use of Silicon Isotope Composition of Biogenic Silica as a Proxy for Environmental Change, Silicon, 1, 65-77, 10.1007/s12633-009-9014-2, 2009.

Mackay, A. W., Ryves, D. B., Morley, D. W., Jewson, D. H., and Rioual, P.: Assessing the vulnerability of endemic diatom species in Lake Baikal to predicted future climate change: a multivariate approach, Global Change Biology, 12, 2297-2315, 10.1111/j.1365-2486.2006.01270.x, 2006.

Mackay, A. W., Felde, V. A., Morley, D. W., Piotrowska, N., Rioual, P., Seddon, A. W. R., and Swann, G. E. A.: Long-term trends in diatom diversity and palaeoproductivity: a 16 000-year multidecadal record from Lake Baikal, southern Siberia, Clim Past, 18, 363-380, 10.5194/cp-18-363-2022, 2022.

Maier, E., Chapligin, B., Abelmann, A., Gersonde, R., Esper, O., Ren, J., Friedrichsen, H., Meyer, H., and Tiedemann, R.: Combined oxygen and silicon isotope analysis of diatom silica from a deglacial subarctic Pacific record, Journal of Quaternary Science, 28, 571-581, 10.1002/jqs.2649, 2013.

Makarova, I. V.: Diatomovye vodorosli Rossii i sopredel'nyh stran: iskopaemye i sovremennye. (The diatoms of Russia and adjacent countries: fossil and recent.) Vol. II, issue 3. , St. Petersburg: St. Petersburg State University Publishers, 2002.

Messager, M. L., Lehner, B., Grill, G., Nedeva, I., and Schmitt, O.: Estimating the volume and age of water stored in global lakes using a geo-statistical approach, Nat Commun, 7, 13603, 10.1038/ncomms13603, 2016.

Meyers, P. A.: Organic Geochemical Proxies, in: Encyclopedia of Paleoclimatology and Ancient Environments. Encyclopedia of Earth Sciences Series., edited by: Gornitz, V., Springer, Dordrecht, 659–663, https://doi.org/10.1007/978-1-4020-4411-3_160, 978-1-4020-4551-6, 2009.

Meyers, P. A. and Teranes, J. L.: Sediment Organic Matter, in: Tracking environmental change using lake sediments. Volume 2: Physical and Geochemical Methods., edited by: Last, W. M., and Smol, J. P., Kluwer Academic Publishers, The Netherlands, 239-269, 1402006284, 2001.

Michelutti, N., Cooke, C. A., Hobbs, W. O., and Smol, J. P.: Climate-driven changes in lakes from the Peruvian Andes, Journal of Paleolimnology, 54, 153-160, 10.1007/s10933-015-9843-5, 2015.

Miesner, T., Herzschuh, U., Pestryakova, L. A., Wieczorek, M., Zakharov, E. S., Kolmogorov, A. I., Davydova, P. V., and Kruse, S.: Forest structure and individual tree inventories of northeastern Siberia along climatic gradients, Earth Syst. Sci. Data, 14, 5695-5716, 10.5194/essd-14-5695-2022, 2022.

Moiseeva, A. I. and Nikolaev, V. A.: Diatomovye vodorosli SSSR. Iskopaemye i sovremennye. (The diatoms of the USSR. Fossil and recent.) Vol. II-2. , Leningrad: Nauka, 1992.

Moore, M. V., Hampton, S. E., Izmest'eva, L. R., Silow, E. A., Peshkova, E. V., and Pavlov, B. K.: Climate Change and the World's "Sacred Sea"—Lake Baikal, Siberia, BioScience, 59, 405-417, 10.1525/bio.2009.59.5.8, 2009.

Morley, D. W., Leng, M. J., Mackay, A. W., Sloane, H. J., Rioual, P., and Battarbee, R. W.: Cleaning of lake sediment samples for diatom oxygen isotope analysis, Journal of Paleolimnology, 31, 391-401, 10.1023/B:JOPL.0000021854.70714.6b, 2004.

Mushet, G. R., Laird, K. R., Das, B., Hesjedal, B., Leavitt, P. R., Scott, K. A., Simpson, G. L., Wissel, B., Wolfe, J. D., and Cumming, B. F.: Regional climate changes drive increased scaled-chrysophyte abundance in lakes downwind of Athabasca Oil Sands nitrogen emissions, Journal of Paleolimnology, 58, 419-435, 10.1007/s10933-017-9987-6, 2017.

O'Reilly, C. M., Sharma, S., Gray, D. K., Hampton, S. E., Read, J. S., Rowley, R. J., Schneider, P., Lenters, J. D., McIntyre, P. B., Kraemer, B. M., Weyhenmeyer, G. A., Straile, D., Dong, B., Adrian, R., Allan, M. G., Anneville, O., Arvola, L., Austin, J., Bailey, J. L., Baron, J. S., Brookes, J. D., de Eyto, E., Dokulil, M. T., Hamilton, D. P., Havens, K., Hetherington, A. L., Higgins, S. N., Hook, S., Izmest'eva, L. R., Joehnk, K. D., Kangur, K., Kasprzak, P., Kumagai, M., Kuusisto, E., Leshkevich, G., Livingstone, D. M., MacIntyre, S., May, L., Melack, J. M., Mueller-Navarra, D. C., Naumenko, M., Noges, P., Noges, T., North, R. P., Plisnier, P. D., Rigosi, A., Rimmer, A., Rogora, M., Rudstam, L. G., Rusak, J. A., Salmaso, N., Samal, N. R., Schindler, D. E., Schladow, S. G., Schmid, M., Schmidt, S. R., Silow, E., Soylu, M. E., Teubner, K., Verburg, P., Voutilainen, A., Watkinson, A., Williamson, C. E., and Zhang, G.: Rapid and highly variable warming of lake surface waters around the globe, Geophysical Research Letters, 42, 10.1002/2015gl066235, 2015.

Obu, J., Westermann, S., Bartsch, A., Berdnikov, N., Christiansen, H. H., Dashtseren, A., Delaloye, R., Elberling, B., Etzelmüller, B., Kholodov, A., Khomutov, A., Kääb, A., Leibman, M. O., Lewkowicz, A. G., Panda, S. K., Romanovsky, V., Way, R. G., Westergaard-Nielsen, A., Wu, T., Yamkhin, J., and Zou, D.: Northern Hemisphere permafrost map based on TTOP modelling for 2000–2016 at 1 km2 scale, Earth-Science Reviews, 193, 299-316, 10.1016/j.earscirev.2019.04.023, 2019.

Oksanen, J., Simpson, G., Blanchet, F., Kindt, R., Legendre, P., Minchin, P., O'Hara, R., Solymos, P., Stevens, M., Szoecs, E., Wagner, H., Barbour, M., Bedward, M., Bolker, B., Borcard, D., Carvalho, G., Chirico, M., De Caceres, M., Durand, S., Evangelista, H., FitzJohn, R., Friendly, M., Furneaux, B., Hannigan, G., Hill, M., Lahti, L., McGlinn, D., Ouellette, M., Ribeiro Cunha, E., Smith, T., Stier, A., Ter Braak, C., and Weedon, J. Oksanen, J., Simpson, G. L., Blanchet, F. G., Kindt, R., Legendre, P., Minchin, P. R., et al.: Vegan: Community Ecology Package. R package version 2.6-4: https://CRAN.R-project.org/package=vegan, last access: 14. March 2024.

Opfergelt, S., Eiriksdottir, E. S., Burton, K. W., Einarsson, A., Siebert, C., Gislason, S. R., and Halliday, A. N.: Quantifying the impact of freshwater diatom productivity on silicon isotopes and silicon fluxes: Lake
1080   Myvatn, Iceland, Earth and Planetary Science Letters, 305, 73-82, 10.1016/j.epsl.2011.02.043, 2011.

Pacyna, J. M., Travnikov, O., De Simone, F., Hedgecock, I. M., Sundseth, K., Pacyna, E. G., Steenhuisen, F., Pirrone, N., Munthe, J., and Kindbom, K.: Current and future levels of mercury atmospheric pollution on a global scale, Atmos. Chem. Phys., 16, 12495-12511, 10.5194/acp-16-12495-2016, 2016.

Palagushkina, O., Nazarova, L., and Frolova, L.: Trends in development of diatom flora from sub-recent
1085   lake sediments of the Lake Bolshoy Kharbey (Bolshezemelskaya tundra, Russia), Biological Communications, 64, 244–251, 10.21638/spbu03.2019.403, 2020.

Panizzo, V. N., Swann, G. E. A., Mackay, A. W., Vologina, E., Sturm, M., Pashley, V., and Horstwood, M. S. A.: Insights into the transfer of silicon isotopes into the sediment record, Biogeosciences, 13, 147-157, 10.5194/bg-13-147-2016, 2016.

1090   Panizzo, V. N., Roberts, S., Swann, G. E. A., McGowan, S., Mackay, A. W., Vologina, E., Pashley, V., and Horstwood, M. S. A.: Spatial differences in dissolved silicon utilization in Lake Baikal, Siberia: Examining the impact of high diatom biomass events and eutrophication, Limnology and Oceanography, 63, 1562-1578, 10.1002/lno.10792, 2018.

Panizzo, V. N., Swann, G. E. A., Mackay, A. W., Vologina, E., Alleman, L., André, L., Pashley, V. H., and
1095   Horstwood, M. S. A.: Constraining modern-day silicon cycling in Lake Baikal, Global Biogeochemical Cycles, 31, 556-574, 10.1002/2016gb005518, 2017.

Paterson, A. M., Cumming, B. F., Smol, J. P., and Hall, R. I.: Marked recent increases of colonial scaled chrysophytes in boreal lakes: implications for the management of taste and odour events, Freshwater Biology, 49, 199-207, 10.1046/j.1365-2427.2003.01170.x, 2004.

1100   Pestryakova, L. A., Herzschuh, U., Wetterich, S., and Ulrich, M.: Present-day variability and Holocene dynamics of permafrost-affected lakes in central Yakutia (Eastern Siberia) inferred from diatom records, Quaternary Science Reviews, 51, 56-70, 10.1016/j.quascirev.2012.06.020, 2012.

R Core Team. R: A Language and Environment for Statistical Computing, R version 4.4.1: https://www.R-project.org/, last access: 2024.

1105   Roberts, S., Adams, J. K., Mackay, A. W., Swann, G. E. A., McGowan, S., Rose, N. L., Panizzo, V., Yang, H., Vologina, E., Sturm, M., and Shchetnikov, A. A.: Mercury loading within the Selenga River basin and Lake Baikal, Siberia, Environ Pollut, 259, 113814, 10.1016/j.envpol.2019.113814, 2020.

Roberts, S. L., Swann, G. E. A., McGowan, S., Panizzo, V. N., Vologina, E. G., Sturm, M., and Mackay, A. W.: Diatom evidence of 20th century ecosystem change in Lake Baikal, Siberia, PLoS One, 13,
1110   e0208765, 10.1371/journal.pone.0208765, 2018.

Round, F. E., Crawford, R. M., and Mann, D. G.: The diatoms: biology and morphology of the genera, Cambridge University Press, 1990.

Rühland, K. and Smol, J. P.: Diatom shifts as evidence for recent Subarctic warming in a remote tundra lake, NWT, Canada, Palaeogeography, Palaeoclimatology, Palaeoecology, 226, 1-16,
1115   10.1016/j.palaeo.2005.05.001, 2005.

Rühland, K., Paterson, A. M., and Smol, J. P.: Hemispheric-scale patterns of climate-related shifts in planktonic diatoms from North American and European lakes, Global Change Biology, 14, 2740-2754, 10.1111/j.1365-2486.2008.01670.x, 2008.

Rühland, K., Priesnitz, A., and Smol, J. P.: Paleolimnological Evidence from Diatoms for Recent
1120   Environmental Changes in 50 Lakes across Canadian Arctic Treeline, Arctic, Antarctic, and Alpine Research, 35, 110-123, 10.1657/1523-0430(2003)035[0110:Pefdfr]2.0.Co;2, 2003.

Rühland, K. M., Paterson, A. M., and Smol, J. P.: Lake diatom responses to warming: reviewing the evidence, Journal of Paleolimnology, 54, 1-35, 10.1007/s10933-015-9837-3, 2015.

Rühland, K. M., Paterson, A. M., Keller, W., Michelutti, N., and Smol, J. P.: Global warming triggers the
1125   loss of a key Arctic refugium, Proc Biol Sci, 280, 20131887, 10.1098/rspb.2013.1887, 2013.

Rutkowski, C., Lenz, J., Lang, A., Wolter, J., Mothes, S., Reemtsma, T., Grosse, G., Ulrich, M., Fuchs, M., Schirrmeister, L., Fedorov, A., Grigoriev, M., Lantuit, H., and Strauss, J.: Mercury in sediment core samples from deep Siberian ice-rich permafrost, Frontiers in Earth Science, 9, 718153, 10.3389/feart.2021.718153, 2021.

1130   Ryves, D. B., Juggins, S., Fritz, S. C., and Battarbee, R. W.: Experimental diatom dissolution and the quantification of microfossil preservation in sediments, Palaeogeogr Palaeocl, 172, 99-113, 10.1016/S0031-0182(01)00273-5, 2001.

Saros, J. E. and Anderson, N. J.: The ecology of the planktonic diatom Cyclotella and its implications for global environmental change studies, Biol Rev Camb Philos Soc, 90, 522-541, 10.1111/brv.12120, 2015.

1135   Saros, J. E., Michel, T. J., Interlandi, S. J., and Wolfe, A. P.: Resource requirements of Asterionella formosa and Fragilaria crotonensis in oligotrophic alpine lakes: implications for recent phytoplankton community reorganizations, Canadian Journal of Fisheries and Aquatic Sciences, 62, 1681-1689, 10.1139/f05-077, 2005.

Saros, J. E., Rose, K. C., Clow, D. W., Stephens, V. C., Nurse, A. B., Arnett, H. A., Stone, J. R., Williamson, 1140   C. E., and Wolfe, A. P.: Melting Alpine Glaciers Enrich High-Elevation Lakes with Reactive Nitrogen, Environmental Science & Technology, 44, 4891-4896, 10.1021/es100147j, 2010.

Saros, J. E., Stone, J. R., Pederson, G. T., Slemmons, K. E., Spanbauer, T., Schliep, A., Cahl, D., Williamson, C. E., and Engstrom, D. R.: Climate-induced changes in lake ecosystem structure inferred from coupled neo- and paleoecological approaches, Ecology, 93, 2155-2164, 10.1890/11-2218.1, 2012.

1145   Schmidtbauer, K., Noble, P., Rosen, M., Conley, D. J., and Frings, P. J.: Linking silicon isotopic signatures with diatom communities, Geochim Cosmochim Ac, 323, 102-122, 10.1016/j.gca.2022.02.015, 2022.

Shestakova, A. A., Fedorov, A. N., Torgovkin, Y. I., Konstantinov, P. Y., Vasyliev, N. F., Kalinicheva, S. V., Samsonova, V. V., Hiyama, T., Iijima, Y., Park, H., Iwahana, G., and Gorokhov, A. N.: Mapping the Main Characteristics of Permafrost on the Basis of a Permafrost-Landscape Map of Yakutia Using GIS, Land, 1150   10, 462, 10.3390/land10050462, 2021.

Sivarajah, B., Rühland, K. M., Labaj, A. L., Paterson, A. M., and Smol, J. P.: Why is the relative abundance of Asterionella formosa increasing in a Boreal Shield lake as nutrient levels decline?, Journal of Paleolimnology, 55, 357-367, 10.1007/s10933-016-9886-2, 2016.

Smol, J. P.: The Ratio of Diatom Frustules to Chrysophycean Statospores - a Useful Paleolimnological 1155   Index, Hydrobiologia, 123, 199-208, Doi 10.1007/Bf00034378, 1985.

Smol, J. P. and Douglas, M. S. V.: From controversy to consensus: making the case for recent climate change in the Arctic using lake sediments, Frontiers in Ecology and the Environment, 5, 466-474, 10.1890/060162, 2007.

Smol, J. P. and Stoermer, E. F.: The diatoms: applications for the environmental and earth sciences, 1160   Cambridge University Press, Cambridge, New York, Melbourne, Madrid, Cape Town, Singapore, São Paulo, Dehli, Dubai, Tokyo, Mexico City, 687 pp., 9780521509961, 2010.

Smol, J. P., Wolfe, A. P., Birks, H. J., Douglas, M. S., Jones, V. J., Korhola, A., Pienitz, R., Ruhland, K., Sorvari, S., Antoniades, D., Brooks, S. J., Fallu, M. A., Hughes, M., Keatley, B. E., Laing, T. E., Michelutti, N., Nazarova, L., Nyman, M., Paterson, A. M., Perren, B., Quinlan, R., Rautio, M., Saulnier-Talbot, E., 1165   Siitonen, S., Solovieva, N., and Weckstrom, J.: Climate-driven regime shifts in the biological communities of arctic lakes, Proc Natl Acad Sci U S A, 102, 4397-4402, 10.1073/pnas.0500245102, 2005.

Sochuliakova, L., Sienkiewicz, E., Hamerlik, L., Svitok, M., Fidlerova, D., and Bitusik, P.: Reconstructing the Trophic History of an Alpine Lake (High Tatra Mts.) Using Subfossil Diatoms: Disentangling the 1170   Effects of Climate and Human Influence, Water Air Soil Pollut, 229, 289, 10.1007/s11270-018-3940-9, 2018.

Solovieva, N., Jones, V., Birks, J. H. B., Appleby, P., and Nazarova, L.: Diatom responses to 20th century climate warming in lakes from the northern Urals, Russia, Palaeogeography, Palaeoclimatology, Palaeoecology, 259, 96-106, 10.1016/j.palaeo.2007.10.001, 2008.

1175   Sorvari, S., Korhola, A., and Thompson, R.: Lake diatom response to recent Arctic warming in Finnish Lapland, Global Change Biology, 8, 171-181, 10.1046/j.1365-2486.2002.00463.x, 2002.

Spaulding, S. A., Potapova, M. G., Bishop, I. W., Lee, S. S., Gasperak, T. S., Jovanoska, E., Furey, P. C., and Edlund, M. B.: Diatoms.org: supporting taxonomists, connecting communities, Diatom Research, 36, 291-304, 10.1080/0269249X.2021.2006790, 2021.

1180   Steffen, W., Broadgate, W., Deutsch, L., Gaffney, O., and Ludwig, C.: The trajectory of the Anthropocene: The Great Acceleration, The Anthropocene Review, 2, 81-98, 10.1177/2053019614564785, 2015.

Stevenson, M. A., McGowan, S., Pearson, E. J., Swann, G. E. A., Leng, M. J., Jones, V. J., Bailey, J. J., Huang, X., and Whiteford, E.: Anthropocene climate warming enhances autochthonous carbon cycling

1185   in an upland Arctic lake, Disko Island, West Greenland, Biogeosciences, 18, 2465-2485, 10.5194/bg-18-2465-2021, 2021.

Stieg, A., Biskaborn, B. K., Herzschuh, U., Strauss, J., Lindemann, J., and Meyer, H.: Mercury from sediment short core EN18232-1 of Lake Khamra, SW Yakutia, Siberia, Russia. [dataset], https://doi.org/10.1594/PANGAEA.962973, 2024a.

1190   Stieg, A., Biskaborn, B. K., Herzschuh, U., Strauss, J., Pestryakova, L., and Meyer, H.: Hydroclimatic anomalies detected by a sub-decadal diatom oxygen isotope record of the last 220 years from Lake Khamra, Siberia, Clim. Past, 20, 909-933, 10.5194/cp-20-909-2024, 2024b.

Streets, D. G., Devane, M. K., Lu, Z., Bond, T. C., Sunderland, E. M., and Jacob, D. J.: All-Time Releases of Mercury to the Atmosphere from Human Activities, Environmental Science & Technology, 45,

1195   10485-10491, 10.1021/es202765m, 2011.

Sun, X., Mörth, C.-M., Porcelli, D., Kutscher, L., Hirst, C., Murphy, M. J., Maximov, T., Petrov, R. E., Humborg, C., Schmitt, M., and Andersson, P. S.: Stable silicon isotopic compositions of the Lena River and its tributaries: Implications for silicon delivery to the Arctic Ocean, Geochim Cosmochim Ac, 241, 120-133, 10.1016/j.gca.2018.08.044, 2018.

1200   Sundseth, K., Pacyna, J. M., Pacyna, E. G., Pirrone, N., and Thorne, R. J.: Global Sources and Pathways of Mercury in the Context of Human Health, Int J Environ Res Public Health, 14, 105, 10.3390/ijerph14010105, 2017.

Sutton, J. N., Varela, D. E., Brzezinski, M. A., and Beucher, C. P.: Species-dependent silicon isotope fractionation by marine diatoms, Geochim Cosmochim Ac, 104, 300-309, 10.1016/j.gca.2012.10.057,

1205   2013.

Sutton, J. N., André, L., Cardinal, D., Conley, D. J., de Souza, G. F., Dean, J., Dodd, J., Ehlert, C., Ellwood, M. J., Frings, P. J., Grasse, P., Hendry, K., Leng, M. J., Michalopoulos, P., Panizzo, V. N., and Swann, G. E. A.: A Review of the Stable Isotope Bio-geochemistry of the Global Silicon Cycle and Its Associated Trace Elements, Frontiers in Earth Science, 5:112, 10.3389/feart.2017.00112, 2018.

1210   Swann, G. E. A., Leng, M. J., Juschus, O., Melles, M., Brigham-Grette, J., and Sloane, H. J.: A combined oxygen and silicon diatom isotope record of Late Quaternary change in Lake El'gygytgyn, North East Siberia, Quaternary Science Reviews, 29, 774-786, 10.1016/j.quascirev.2009.11.024, 2010.

Todd, M. C. and Mackay, A. W.: Large-scale climatic controls on Lake Baikal ice cover, Journal of Climate, 16, 3186-3199, Doi 10.1175/1520-0442(2003)016<3186:Lccolb>2.0.Co;2, 2003.

1215   Varela, D. E., Pride, C. J., and Brzezinski, M. A.: Biological fractionation of silicon isotopes in Southern Ocean surface waters, Global Biogeochemical Cycles, 18, GB1047, 10.1029/2003gb002140, 2004.

Verburg, P.: The need to correct for the Suess effect in the application of δ13C in sediment of autotrophic Lake Tanganyika, as a productivity proxy in the Anthropocene, Journal of Paleolimnology, 37, 591-602, 10.1007/s10933-006-9056-z, 2007.

1220   Wang, Q., Kim, D., Dionysiou, D. D., Sorial, G. A., and Timberlake, D.: Sources and remediation for mercury contamination in aquatic systems--a literature review, Environ Pollut, 131, 323-336, 10.1016/j.envpol.2004.01.010, 2004.

Winder, M. and Sommer, U.: Phytoplankton response to a changing climate, Hydrobiologia, 698, 5-16, 10.1007/s10750-012-1149-2, 2012.

1225   Wolfe, A. P., Hobbs, W. O., Birks, H. H., Briner, J. P., Holmgren, S. U., Ingólfsson, Ó., Kaushal, S. S., Miller, G. H., Pagani, M., Saros, J. E., and Vinebrooke, R. D.: Stratigraphic expressions of the Holocene–Anthropocene transition revealed in sediments from remote lakes, Earth-Science Reviews, 116, 17-34, 10.1016/j.earscirev.2012.11.001, 2013.

Woolway, R. I., Kraemer, B. M., Lenters, J. D., Merchant, C. J., O'Reilly, C. M., and Sharma, S.: Global

1230   lake responses to climate change, Nature Reviews Earth & Environment, 1, 388-403, 10.1038/s43017-020-0067-5, 2020.

Zahajská, P., Olid, C., Stadmark, J., Fritz, S. C., Opfergelt, S., and Conley, D. J.: Modern silicon dynamics of a small high-latitude subarctic lake, Biogeosciences, 18, 2325-2345, 10.5194/bg-18-2325-2021, 2021a.

1235   Zahajská, P., Cartier, R., Fritz, S. C., Stadmark, J., Opfergelt, S., Yam, R., Shemesh, A., and Conley, D. J.: Impact of Holocene climate change on silicon cycling in Lake 850, Northern Sweden, The Holocene, 31, 1582-1592, 10.1177/09596836211025973, 2021b.